Hybrid filler systems in rubber nanocomposites

11

M. Galimberti[1], *S. Agnelli*[2] *and V. Cipolletti*[3]
[1]Politecnico di Milano, Milano, Italy, [2]University of Brescia, Brescia, Italy, [3]Pirelli Tyre, Milano, Italy

11.1 Introduction

11.1.1 Objective and structure of the chapter

Reinforcing fillers used at the commercial level in rubber compounds, such as carbon black (CB) and silica, are nanostructured: they are made by aggregates of spherical primary particles that can not be separated by thermomechanical mixing [1]. On the contrary, nanofillers [2,3] have primary particles with at least one dimension below 100 nanometers [4], that can be individually dispersed in the rubber matrix. In recent decades, nanofillers are one the most important novelties in the rubber field. The three main families of nanofillers are the subject of large research efforts in academic and industrial laboratories and have already found commercial applications: clays (C) and organically modified clays (organoclays, OC), [2,3,5−10], carbon nanotubes (CNTs), [2,3,11] and graphene (G) or graphitic nanofillers made by a few layers of graphene (named as graphite nanoplatelets (GNPs), nanosheets, or nanoflakes) [3,12−16].

It is nowadays clear that nanofillers can hardly replace the nanostructured ones in large-scale applications. However, the combination of both families of fillers can lead to remarkable properties.

This chapter is dedicated to rubber composites based on the combination of nano- and nano-structured fillers. It makes reference to what has been published in the scientific literature but it is not a directory of what is available. In fact, it is mainly focused on systems that have been remarkably investigated in the literature and that have already found some commercial applications. They are those based on CB and either OC or CNT or nanographite. Systems based on silica and CNT are also considered. For other families of combinations, in particular, combinations of nanofillers, that have been studied only to a minor extent, reference is given to the specific literature.

In particular, the authors' intention was to analyze synergistic effects of hybrid fillers, with the aim to model them. Results reported in the literature are based on a large variety of fillers, polymer matrices, as well as experimental conditions. This does not allow to attempt an overall rationalization. However, at the end of the chapter, a model proposed by the authors for the rationalization of the mechanical reinforcement is discussed.

Progress in Rubber Nanocomposites. DOI: http://dx.doi.org/10.1016/B978-0-08-100409-8.00011-5

11.1.2 Hybrid filler systems?

Words are important in the scientific field. They have semantic implications and, most of all, they should be used correctly. How to define filler systems made by the combination of nano- and nanostructured fillers? In most papers, authors use the expression "hybrid filler system." Is this expression correct? Or should it be more appropriate to use dual filler or three phase composite? The term "hybrid" commonly means something composed of mixed parts and, to the authors' opinion, the definition "hybrid filler system" gives an added value to the concept of a three phase composite. In fact, the term "hybrid" underlines that the two different fillers are intentionally added together to the matrix to obtain specific properties and, if possible, synergistic effects between the two fillers.

The IUPAC definition of "hybrid material" [17] is a "material composed of an intimate mixture of inorganic components, organic components, or both types of component." An important note states that "the components usually interpenetrate on scale of less than 1 μm." In the light of this definition, systems based on nano- and nanostructured fillers can be defined as "hybrid filler systems."

Different definitions of hybrid material are given and revised in literature [18]: some of them relate to the submicrometer size of the mixing, some others are more focused on the creation of new chemical bonds or new functions. A new systematic classification of hybrid materials is proposed [18], which includes three categories, depending on the purpose of the mixing of materials:

1. "structurally-hybridized materials," when the purpose of the combination or mixture of materials is hybridization of the macroscopic structure;
2. "materials hybridized in chemical-bond," when the purpose of mixing is the creation of new chemical bonds between different materials in order to obtain superior performance and/or new functions in the hybrid materials;
3. "functionally-hybridized materials," when the aim is the creation of new functions or super functions.

Nanocomposites are therefore included at least in the first definition, if not in the second one, when chemical bonds at the interface between the component materials play a key role in material development.

A specific definition has not been established, yet, for rubber composites filled with at least two different fillers or nanofillers. As a consequence, different expressions are reported in the literature works reviewed in this chapter. The authors of this chapter propose to refer to these materials as "hybrid filler systems," but, the terms used by the literature will be uncritically reported, trying to clarify the author's choice of terminology.

11.1.3 Synergistic effects of different fillers on the properties of rubber composites

The challenging goal of the research activity on hybrid filler systems is to develop synergistic effects between two different fillers, achieving substantial improvement

of the material properties. In spite of such a stimulating goal, only a few works in the literature explicitly point out synergistic effects. Moreover, such effects are addressed only qualitatively and are not quantified.

According to the common definition, e.g., reported in the Oxford dictionary, a synergistic effect arises from the interaction or cooperation of two or more substances and leads to produce a combined effect greater than the sum of the substances separate effects. This definition holds also in the case of polymer composites: in this case, fillers are the substances. To realize the occurrence of a synergistic effect, it is crucial to define to what extent it should be greater the effect arising from the cooperation of different substances. In the literature, synergistic effects are defined in different ways. Most of them refer to the higher properties obtained in hybrid filled systems in comparison to systems containing only the nanostructured filler at the same overall filler amount [19−22]. Other authors compare hybrid and single-filler systems with different filler amounts but having the same level of a specified property, such as hardness [23] or tensile properties [24]. Synergistic effects are also claimed when a nanofiller is added to a composite containing a given amount of nanostructured filler. In this chapter, the synergistic effects explicitly reported in the literature works will be quoted, along with the criterion used to establish them.

An attempt to quantify synergistic effects (cautiously defined "interactive effects") on the initial modulus of rubber composites has been reported only by Agnelli et al. [25]. Elaboration of such an attempt is discussed below in the chapter.

11.1.4 Self-assembly of nanofillers in rubber matrix

In the prior art, aggregation and self-assembly have been first associated with micellar and colloidal systems and then also with molecules systems, as a consequence of the advent and success of supramolecular chemistry. Synonyms are adopted to describe self assembly: self-organization, molecular self-assembly, dynamic self-assembly. To rationalize the terminology, IUPAC came out with "Terminology for aggregation and self-assembly in polymer science" (IUPAC Recommendations 2013). In [26], it is reported that self assembly is the spontaneous and reversible organization of molecular entities by noncovalent interactions, where typical noncovalent interactions are van der Waals interactions, $\pi-\pi$ interactions, electrostatic interactions, and hydrogen bonds. Note 2 appears particularly interesting in the light of what reported in this chapter, as it reports that self-assembly is a process in which a system of preexisting components, under specific conditions, adopts a more organized structure through interactions between the components themselves. Indeed, the organization of fillers in a rubber matrix plays a dominant role for the final properties of the composite materials.

In the light of what is defined by IUPAC and reported in the literature, it can be said that the self-assembly of fillers indicates the driving mechanism for the aggregation of fillers in a solvent that steers its spatial arrangement. To achieve a controlled filler dispersion in polymer matrix composites, different self-assembly mechanisms can be exploited, which are driven by different forces: shear-flow forces [27] in blending methods, and physical interactions among particles, such as

electrostatic attraction, hydrophobic interactions, and H bonding [28]. In rubber matrices, self-assembly methods were used to achieve uniform dispersion in NR latex of CNT [28] and of chemically reduced graphene [29], also achieving some degree of orientation.

Self-assembly of hybrid fillers is not explicitly addressed in the literature on rubber composites. However, as it will be pointed out below in the text, interaction between nano- and nanostructured fillers is clearly documented. The presence of the second filler might be thus a driving force for self-assembly. Hybrid nanofillers can exert synergistic effects that lower the percolation threshold [30]. The lower percolation threshold of nanofillers was clearly documented in the presence of CB, in the case of organoclay, CNTs, and nano-sized graphite [31], even though the phenomenon of self-assembly was not explicitly mentioned. In [32] the interaction between alumina and clay in cross-linked polyethylene gave rise to a unique filler architecture. In polyacrylonitrile nanofibers [33], self-assembly of montmorillonite/graphene oxide (GO) hybrid nanofillers led to improved properties due to the mutual-assisted dispersion of the two fillers in solvent. In a polyamide-6 [34], percolation threshold substantially shifted to lower CB contents in the presence of organoclay, since organoclay acted like a dispersion control agent to induce self-assembly of CB network. As discussed below in the text, OC and CB were reported to create "nanounits."

11.2 Nanocomposites based on organoclays and carbon black

A good number of papers are available in the scientific literature on rubber nanocomposites based on OC and CB. They are collected in Table 11.1, that shows the type of rubber, CB and OC, the blending technology, and the main aspects investigated in the work.

11.2.1 Structure of OC–CB nanocomposites

In the literature, the structure of nanocomposites based on CB and OC has been investigated by means of transmission electron microscopy (TEM), scanning electron microscopy (SEM), and X-ray diffraction (XRD).

11.2.1.1 OC organization in the rubber matrix

A clay mineral, pristine or modified with cations different from the naturally occurring ones, has a multiscale organization in a polymer matrix. Clay minerals are layered: they can be present in the rubber matrix as individual layers or in stacks. This is the lowest level of clay organization. Distribution and dispersion of clay aggregates are at the upper level of clay organization. Moreover, clays are made by platelets with high aspect ratio that can be oriented in the rubber matrix, as a consequence of different process conditions.

Table 11.1 Papers on OC−CB hybrid fillers: type of rubber, CB and OC, blending technology and main aspects investigated in the work

References	Rubber	CB type	OC type	Blending method	Analyses
[35]	E-SBR (S = 23.75%) Buna VSL 5025-2	N234	Cloisite C20A: 2HT	Emulsion blending for masterbatch. Melt blending	TEM, XRD, cure properties, dynamic-mechanical analysis (strain sweep and temperature sweep in tensile mode), tensile test, tear test, Shore A hardness
[36]	IR	N326	Dellite 67G: 2HT	Melt blending	XRD, TEM, DSC, dynamic-mechanical analysis (shear sandwich mode, strain sweep, recovery test, master curve on uncrosslinked material)
[37]	BIMS	N660	Cloisite C20A: 2HT	Melt blending	TEM, SAXS, permeability
[38]	CR	N550	Cloisite 15A: 2HT	Melt blending	TEM, XRD, cure characteristics (by MDR), tensile test, tear test, electrical properties
[39]	ENR25	N330	Cloisite 30B: T $(CH_2CH_2OH)_2$	Melt blending (two roll mill)	SAXS, High resolution TEM, swelling, tensile test, dynamic-mechanical analysis (temperature sweep in tensile mode)
[22]	IR	N326	Mt/2HT	Melt blending	TEM, mooney viscosity, DSC, bound rubber, density, cure characteristics (by MDR), dynamic-mechanical analysis (strain sweep in shear mode)
[40]	ESBR 1502 (S = 23) XSBR	N774	Cloisite 15A: 2HT Cloisite 20 A: 2HT Cloisite 30B: T $(CH_2CH_2OH)_2$	Solution blending XSBR for masterbatch. Melt blending with E-SBR	Cure characteristics (by MDR), WAXD High resolution TEM, SEM, TGA, dynamic-mechanical analysis (temperature sweep in tensile mode), tensile test, tear test

(*Continued*)

Table 11.1 (Continued)

References	Rubber	CB type	OC type	Blending method	Analyses
[41]	ESBR 1502 (S = 23)	N330	Cloisite 20A: 2HT	Melt blending	SAXS, FTIR, high resolution TEM, tensile test, tear test, abrasion test, heat build up, dynamic-mechanical analysis (temperature sweep in tensile mode, frequency and strain sweep in shear mode)
[42]	NR	N234	Clay Rockwood + 2HT or ODA	Melt blending	XRD, mooney viscosity, cure characteristics and kinetics, dynamic-mechanical analysis (strain sweep in shear mode), tensile test, hardness
[43]	X-NBR	N330	Nanomer I30E: ODA	Melt blending (two roll mill)	WAXD, TEM, curing characteristics, tensile test
[44]	IR	N326	Dellite 67 G: 2HT	Melt blending	Curing characteristics (by ODR), TEM, WAXD, density, tensile tests, dynamic-mechanical analysis (strain sweep in shear mode)
[45]	EPDM: E/P = 6/4, ENB = 9.4 XSBR	N774	Cloisite 15A: 2HT Cloisite 30B: T $(CH_2CH_2OH)_2$	Solution blending XSBR + Clay. Melt blending with EPDM	Curing characteristics, XRD, high resolution TEM, SEM, dynamic-mechanical analysis (temperature sweep in tension mode), tensile test, TGA
[46]	ENR	N550, N330, N220, N110	Nanomer I30E ODA	Melt blending	SAXS, high resolution TEM, dynamic contact angle, dielectric measurements, AC resistance, volume resistivity, tensile test Dynamic-mechanical analysis (temperature and strain sweep in tension mode)

[47]	E-SBR 1502	N330	Cloisite 15A: 2HT	Melt blending (two roll mill)	XRD, TEM, tensile test, dynamic-mechanical analysis, heat build up, abrasion test
[48]	NR	N330, N754	Closite 15A: 2HT Cloisite 20 A: 2HT	Melt blending (two roll mill)	TEM, SEM, tensile test, tear test, fatigue test
[24]	NR (SMR)	N330	Mt/Distearyl	Melt blending	XRD, TEM, cure characteristics, tensile test, Shore A hardness, dynamic-mechanical analysis (temperature sweep in tension mode)
[49]	IR, NR, BR, E-SBR 1721, S-SBR SOL R72612, Buna 5025-0	N326	Dellite HPS, Dellite 67G: 2HT	Melt blending	XRD, TEM, Mooney viscosity, cure characteristics (by MDR), tensile test, hardness, dynamic-mechanical analysis (temperature sweep in tensile mode)
[50]	E-SBR-1502	N330	Nanomer I30E: ODA	Melt blending (two roll mill)	XRD, TEM, tensile test, dynamic-mechanical analysis (temperature sweep in tensile mode)
[15]	Chlorobutyl, CIIR	N330	Cloisite 15 A: 2HT	Solution blending Rubber + clay Melt blending Masterbatch + CB	curing characteristics (by ODR), tensile test, tear test, Shore A hardness, dynamic-mechanical analysis (temperature sweep in tensile mode), positron annihilation, bound rubber
[51]	SIR20 E-SBR 1712	N339	Mt/ tetraalkylammonium	Solution blending Rubber + clay Melt blending Masterbatch + CB	FT-IR, curing characteristics, tensile test, tear test, abrasion test, heat build up, De Mattia crack initiation test
[52]	poly(isobutylene-co paramethylstyrene) styrene-butadiene rubber	N330, N550, N660	ODA	Solution blending	XRD, tensile test, dynamic-mechanical analysis (temperature sweep in tensile mode)

11.2.1.2 Lowest level of clay organization: stacking or exfoliation

As it will be shown below, in most of the TEM micrographs available in the papers of Table 11.1, both individual lamellae and tactoids made by few layers are visible. Comments are proposed on what is intercalated in the space available between two opposite layers: only the ammonium cation or also the polymer chains? In the scientific literature, many reports are available on this point [5,6,53] for rubber clay nanocomposites in the absence of CB. In order to rationalize the clay organization in the rubber matrix in the presence of CB, it is worthwhile to take this literature into consideration and, in particular, it is useful to summarize the crystalline organization of pristine OC, prior to the mixing with the rubber. In fact, as it will be discussed below, the presence of CB does not substantially alter the situation.

Fig. 11.1A shows the XRD patterns of Na-Mt: (a) pristine; (b) modified with T (2-hydroxyethyl); and (c) 2HT. Fig. 11.1B shows the structure of the organophilic cations used in the papers of Table 11.1 for clay modification.

In the XRD pattern, (00ℓ) indexes refer to a crystalline order in the direction perpendicular to the structural layers: (001) reflection is due to regularly stacked layers whereas higher order reflections, e.g., (002) and (003), originate from the regular arrangement of intercalants. An expansion of d interlayer spacing corresponds to a shift of (001) reflection towards lower 2θ angle values. In Fig. 11.1A, it is evident that the intercalation of organophilic cations leads to expansion of interlayer distance and to the appearance of higher order reflections in the XRD pattern, when the ammonium cation has long chain substituents such as 2 talloyl groups.

Meaningful data on the organization in the interlayer space have been recently proposed [54]. Reaction of Mt with 2HTCl was performed either at the solid state in the absence of any other chemical substance, or in the presence of solvents, or in

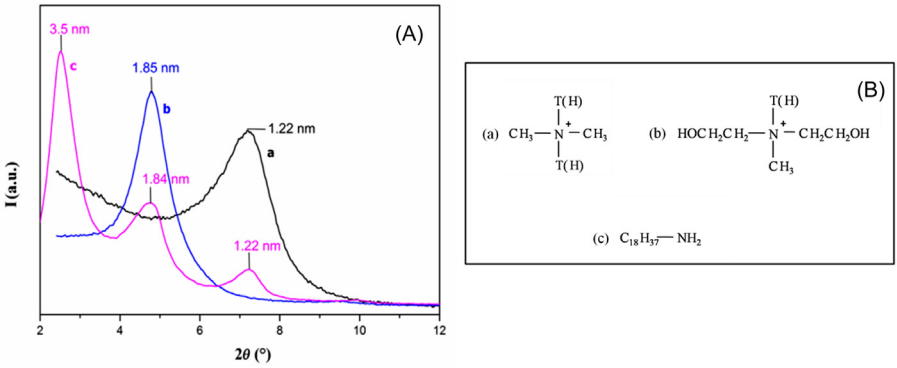

Figure 11.1 (A) XRD patterns of Na-Mt: pristine (Cloesite®) (a), modified with T(2-hydroxyethyl) (Cloesite® 30B) (b), 2HT (Dellite® 67 G) (c). (B) organophilic clay compensating cations: 2HT (a), T(CH_2CH_2OH)$_2$ (b), ODA (c).
Source: Reprinted with permission from Galimberti M. Rubber clay nanocomposites: science, technology, applications, 1st ed., John Wiley and Sons; 2011.

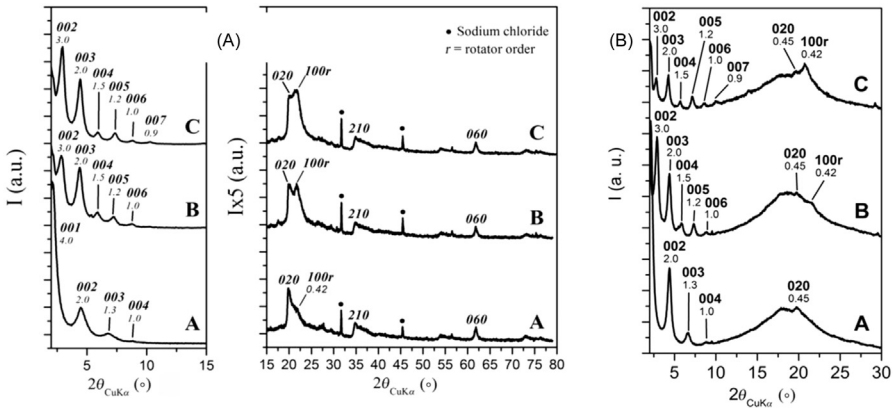

Figure 11.2 XRD patterns of: (A) (a) Mt/2HT, (b) Mt/2HT/SA, (c) Mt/2HT/SAES, prepared from neat synthesis. Asterisks indicate reflections due to NaCl and symbol *r* indicate reflections relative to the rotator order; (B) OC samples prepared in IR as the reaction medium: (a) Mt/2HT, (b) Mt/2HT/SA, (c) Mt/2HT/SAES.
Source: Reprinted with permission from Cipolletti V, Galimberti M, Mauro M, Guerra G. Organoclays with hexagonal rotator order for the paraffinic chains of the compensating cation. Implications on the structure of clay polymer nanocomposites. Appl Clay Sci 2014;87:179−88.

poly(1,4-cis-isoprene) as the reaction medium, optionally adding either stearic acid (SA) or 2-stearamidoethyl stearate (SAES). In Fig. 11.2A, the XRD patterns of OC samples prepared through neat synthesis, in the absence of solvents, reveal two interlayer distances: 3.6−4.0 nm for Mt/2HT and about 6 nm for Mt/2HT/SA and Mt/2HT/SAES. The 3.6−4 nm value was explained with the bilayer placement of the tilted paraffinic chains of the ammonium cation [55] and the 6 nm value with the perpendicular placement of the paraffinic chains, associated with the presence in the interlayer space of either the acid or the amide. For the first time, it was documented the occurrence of hexagonal rotator order in the packing of the long hydrocarbon tails of the 2HT compensating cation. SA and, in particular, SAES were found to enhance this type of order. Fig. 11.2B shows XRD patterns of OC samples prepared in IR as the reaction medium: (A) Mt/2HT, (B) Mt/2HT/SA, (C) Mt/2HT/SAES. Exactly the same reflections were obtained for crystalline OC and the rotator order was detected.

These findings demonstrate that low molecular mass chemicals are able to get in the interlayer space, together with the compensating cation, leading to a further expansion of the interlayer distance. Moreover, they demonstrate that the same OC crystalline structures are formed in the absence and in the presence of polymer chains, thus suggesting that polymer intercalation is not such a likely phenomenon as it is widely considered in the literature. The maximum value reported in the literature, for the interlayer distance of crystalline OC, is 6 nm. XRD analysis on composites of Table 11.1 was performed on polymer composites containing low molecular mass chemicals and d_{001} spacing is, in all papers, well below 6 nm.

Hence, it is hard to state who is to blame for the expansion of the interlayer distance. However, the objective of this paragraph is to assess if CB plays a role in modifying the OC organization in the polymer matrix.

Some papers indicate a minor influence, if any, by CB on the clay organization in the interlayer space. Reflections due to OC(2HT), in XRD patterns of composites based on IR and containing CB, were found at the same 2θ values [36,44] as in XRD patterns of pristine OC. In NR as the matrix, the expansion of the OC interlayer distance was substantially a function of the low molecular mass guests in the interlayer space; it was larger for 2HT than for ODA [42], whereas OC(2HT) exfoliation was promoted by preparing an "expanded clay," by intercalating a long chain fatty acid together with the ammonium cation [24]. Expansion of interlayer distance was found by preparing OC(2HT)/E-SBR blend through latex blending [35], and the expansion of the interlayer distance was absent or very minor after melt blending with S-SBR/BR and CB. The XRD patterns of nanocomposites (OC with 2HT) based on BIMS and CB had general features that were similar to those of nanocomposites without CB [37]. In XNBR matrix, the key role for the OC(ODA) organization was played by a low molar mass liquid rubber, carboxyl-terminated copolymer of butadiene and acrylonitrile, rather than by CB [43]; the intercalation of the liquid rubber led to further expansion and exfoliation of OC.

Only a minor number of reports suggest an effect of CB for clay intercalation. In the case of silicone butadiene rubber (SBR) based nanocomposites (OC with ODA), further expansion of the interlayer distance was observed in the presence of CB and was attributed to the enhancement of polymer intercalation [50]. For composites based on CR, addition of CB was reported to favor OC(2HT) dispersion and intercalation [38]. In the case of composites based on ESBR and OC(2HT), the addition of calcium stearate led to a further expansion of the interlayer distance, that was attributed to the specific ionic interaction existing between anionic surface of layered silicates and Ca^{2+} and interpreted with a more pronounced intercalation [41].

The effect of CB on OC exfoliation seems to be different, in different papers. The addition of CB to composites based on BIMS hindered the OC(2HT) exfoliation process (unfunctionalized BIMS) or at least did not enhance the exfoliated structure (functionalized BIMS) [37].

Composites based on either E-SBR [40] or EPDM [45] and CB did not reveal reflections due to OC. However, OC was first dispersed in a masterbatch with carboxylated styrene butadiene rubber (XSBR) via solution blending. In ENR25 the exfoliation of OC(ODA, T2HE) was found to depend on the compensating cation. It was reported that the interactions between CB and OC(ODA) were more intimate than that of CB and OC(2THE) and such larger interactions led to larger exfoliation [39].

11.2.1.3 Upper level of clay organization: distribution and dispersion of OC

Both CB and OC achieve better dispersion in composites based on the binary CB−OC system. In fact, CB was reported to favor OC (ODA) dispersion, through

the formation of the so-called "nanounit" [50]. Prevailingly delaminated OC(2HT) was observed to promote a remarkable improvement of CB dispersion [22,44].

OC distribution and dispersion in rubber matrices with CB are affected by the nature of the polymer matrix, by the blending technology, by the degree of OC exfoliation, and by the addition of promoters of dispersion. The overall OC(2HT) distribution was reported to be homogenous in rubber composites based on an apolar matrix such as the isoprene rubber [36,44]. Dispersion of OC, with larger exfoliation, was improved by using a polar Mt modifier, such as T2HE instead of 2HT, for the preparation of masterbatches with a polar rubber such as XSBR [40]. When a masterbatch of OC in E-SBR was prepared via latex blending, the successive melt blending in BR led to a good OC dispersion [35].

OC exfoliation was reported to favor the homogenous clay distribution. In [39], composites were compared, based on HNR-25, CB N330, and either OC(ODA) or OC(T2HE). A larger degree of exfoliation was achieved with ODA as the modifier and clay dispersion was observed to be more uniform.

Calcium stearate has been reported to act as a dispersion promoter for OC(2HT) in SBR matrix [41].

11.2.1.4 Orientation

Orientation of OC(2HT) in nanocomposites based on BIMS was studied as a function of the type of flow [37]. In the extrusion flow, the extensional component aligned the organoclay particles along the flow direction and the squeeze flow of the melt compression process aligned the sheet-like organoclay particles along the planar direction. In the case of unfunctionalized BIMS, in spite of the tendency of clays to wrap around CB particles, most clay tactoids maintained large axial orientation and they did not curve notably. When BIMS was functionalized, either with triethylamine or with dimethyl benzoic acid, the presence of CB decreased the organoclay orientation parallel to the plane direction of the polymer film.

In IR based composites processed through a two roll mill and pressed for the vulcanization step [22], isolated silicate layers or stacks (OC with 2HT) appeared in TEM micrographs oriented along a preferential direction.

In HNBR, with either 5 or 15 phr of CB [56] and OC(2HT) either in place of the 5 CB phr or added to the 15 CB phr, the mechanical properties of nanocomposites could be explained by the formation of an anisotropic, oriented filler–filler network.

11.2.1.5 Fractured surfaces

Tensile fractured surface of hybrid nanocomposites showed highly rougher surface morphology compared to the composites based on rubber, either neat or containing OC. This was attributed to the dispersion of CB and OC(ODA, T2HE) platelets in the rubber matrix, that alter the crack path depending upon their orientation [45].

11.2.2 Affinity of OC for CB

TEM micrographs demonstrate that OC have affinity for CB; OC individual layers and tactoids lie close to CB particles. It is reported that OC and CB form hybrid filler networks. These findings are independent of the type of polymer matrix and clay modifier.

Fig. 11.3a,B show TEM micrographs of nanocomposites based on IR [44] and BIMS [37] as the polymer matrix and OC with 2HT as the compensating cation.

In the micrographs of Fig. 11.3, individual lamellae and tactoids can be detected, for both nanocomposites. As reported in [37], the majority are observed around CB clusters, with only a small fraction laying in the polymer matrix.

In NR matrix [48] physical contact network between OC(2HT) and CB was observed, with clay layers bridging CB aggregates, and the formation of a hybrid network was also proposed. Favorable interaction between CB and OC(2HT) has been observed also in CR [38].

OC(ODA) and CB were reported to form a dual structure, named a "nanounit," in E-SBR 1502 [50] and in ENR [39,46]. As mentioned by the authors of these papers, the OC−CB "nanounit" was first found in polyamide-6/OC(2T2HE)/CB ternary hybrids [34]. The nanounit was described as composed of stacked clay platelets that deform to wrap partially around one or two primary CB aggregates. This elementary nanounit structure induced self-assembly of a CB network within polyamide 6 matrices. Such a structure was prevalent throughout the polymer matrix and remained robust under a wide range of thermal deformation histories.

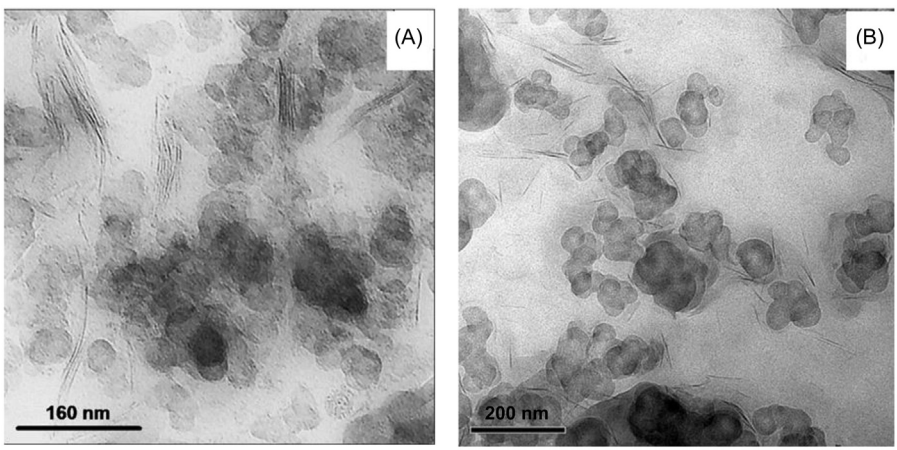

Figure 11.3 TEM micrographs of OC−CB composites: (A) IR as the polymer, N326 as CB, 7.5 as OC phr, 2HT as the cation; (B) BIMS as the polymer, N660 as CB, 2HT as the cation. *Source*: For (A) Reprinted with permission from Galimberti M, Coombs M, Cipolletti V, Riccio P, Ricco T, Pandini S, et al. Enhancement of mechanical reinforcement due to hybrid filler networking promoted by an organoclay in hydrocarbon based nanocomposites. Appl Clay Sci 2012;65−66:57−66. For (B) Reprinted with permission from Nawani P, Burger C, Rong L, Hsiao BS, Tsou AH. Structure and permeability relationships in polymer nanocomposites containing carbon black and organoclay. Polymer (Guildf) 2015;64:19−28.

The effect of OC organization on the formation of the hybrid filler structure was investigated [36]. OC(2HT) was delaminated through ball milling and composites based on IR and OC, either pristine or delaminated, were prepared. As revealed by TEM micrographs, the larger volume occupied by pristine OC stacks helped to form bridges between CB clusters, whereas individual clay layers obtained via ball milling simply adhered to CB particles.

11.2.2.1 The origin of the affinity of OC for CB

In the case of nanocomposites in nylon 6 matrix [34], the attraction of CB toward the organoclay platelet was explained with a combination of weaker (London dispersion forces) and stronger (hydrogen bonding) interactions between the amide group of nylon 6 chains, negatively charged pristine clay and functional groups attached to the organic modifier. It was written that competitive adsorption on CB rough surfaces occurs between the end tail sides of nylon 6 chains and organoclay. Thanks to the improved CB dispersion, the electrical CB percolation threshold was substantially shifted to lower volume fractions.

The dispersion of CB was found to be dramatically improved in IR as the matrix in the presence of only the ammonium salt 2HTCl. The favorable interaction between the organophilic cation and CB was explained with the cation-pi interaction, well known in organic chemistry, that was thus proposed at the origin of OC−CB affinity [22]. Such favorable interaction is well documented in the scientific literature.

Even distribution of OC and CB should be expected also on the basis of the Zeta potential (ZP) values of nanoparticles [57]. ZP is the measure of the repulsion between particles that are similarly charged. In rubber composites, ZPs of nanofillers, at typical pH levels, are negative, whereas ZPs of CBs are positive [58−62]. ZP can be applied also to highly viscous nonaqueous fluids, such as polymer melts. In the case of CB hybrid systems with clays, studies are reported on clay bonhomie [63,64].

11.2.3 Curing

Curing of nanocomposites based on OC and CB of Table 11.1 was performed with sulfur based systems.

It is widely acknowledged that CB promotes acceleration of curing reactions of diene rubbers, promoted by sulfur [65,66]. Explanations are based on the increased thermal conductivity of the compound as well as on the supposed basic pH of CB.

OC also gives rise to faster curing [2,67−69]. The formation of amines from the ammonium cations and the increased mobility of sulfur accelerating anionic species are considered to be at the origin of this phenomenon [70].

Results available in the papers of Table 11.1 demonstrate that the addition of OC, to rubber composites containing CB, brings faster curing, with reductions of scorch and optimum times of vulcanization. This is reported for many different systems, such as NR-OC(2HT, ODA) [42] NR-OC(2HT) [24], IR-OC(2HT) [44], SBR-OC(2HT) [41], XNBr-OC(ODA) [43], NR/BR blend (OC with quaternary ammonium) [51], and EPDM-OC(2HT, T2HE) [45].

Results are also available that show a synergistic effect of OC and CB: in CR matrix [38], lower scorch time was observed for the composite with the hybrid filler system with respect to those based on only either CB or OC(2HT). A prevulcanization inhibitor, such as a thiophtalimide, was proved to be efficient for controlling the reduction of scorch time [44].

The ammonium cation acts thus as an accelerator, but the curing reaction relies on the traditional ingredients, such as, e.g., divalent Zn cations. In fact, the addition of a small amount of calcium stearate to composites containing ZnO [41] led to a further increase of curing rate, thanks to the formation of soluble Zn soap, whereas further addition deactivated the reaction, capturing zinc.

The value of the maximum modulus depends on the amount of OC. M_H increases for low OC values and then decreases, for OC(2HT, ODA) [42], OC (2HT) [24], (OC with quaternary ammonium) [51] or reaches a plateau value for OC(2HT) [44]. The decrease of M_H value after a given amount of OC is explained with the plasticizing effect of the long alkyl chain substituents of the ammonium cations. Plasticization can be also due to other OC modifiers, such as the carboxyl-terminated copolymer of butadiene and acrylonitrile used to compatibilize OC (ODA) with carboxylated acrylonitrile–butadiene rubber matrix [43] or the SA used to prepare the so-called expanded OC(2HT) [24]. Larger values of M_H were also ascribed to different dispersions of OC in the matrix: e.g., in EPDM [45], OC with T2HE was reported to be better dispersed than OC with 2HT.

Swelling measurements, performed on ENR based nanocomposites [39] revealed that OC(T2HE) helped the swelling, however, in the presence of poor OC dispersion.

11.2.4 Mechanical reinforcement as a function of fillers' features

Reinforcement of a rubber is obtained when a filler(s) with a much higher modulus is added to the soft matrix. According to theories developed for *98 InTech* CB as the filler, the modulus of a filled rubber compound can be seen as the sum of different contributions, as it is shown in Fig. 11.4.

Contributions that do not depend on the strain amplitude are due to the polymer network, hydrodynamic effects, and immobilization of rubber on filler particles. The contribution that depends on the strain amplitude is the so-called filler network: filler particles are joined together either directly or through polymer layers. To describe mechanical reinforcement, micromechanical models have been developed [1,71,72] based on the replacement of part of the soft matrix with filler particles, that take into account the nonlinear dependence of the modulus on the filler concentration as the result of interactions of stress fields of each filler particle. The Smallwood–Guth–Gold equation (Eq. (11.1)) [73] expresses the enhancement of the matrix elastic modulus as a function of volume fraction of the added filler:

$$G_c G_c / G_m = 1 + 2.5\Phi + 14.1\Phi^2 \tag{11.1}$$

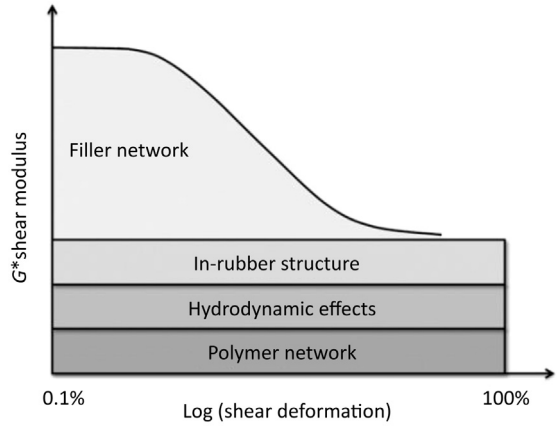

Figure 11.4 Modulus of a rubber compound filled with a particulate filler as the sum of different contributions.
Source: From Galimberti M. Rubber clay nanocomposites: science, technology, applications. 1st ed. John Wiley and Sons; 2011.

where G_c and G_m are the elastic moduli of the composite and of the neat elastomer, respectively, Φ is the filler volume fraction and the quadratic term accounts for the mutual disturbance of filler particles. For particle aggregates and for nonspherical particles, another equation was proposed by Guth [74] (Eq. (11.2)):

$$G_c/G_m = 1 + 0.67f\Phi + 1.62f^2\Phi^2 \tag{11.2}$$

where f is the shape factor, given by the length to width ratio of aggregate or particle. To take into account the occlusion of rubber in the filler voids, Φ is replaced by Φc, calculated through measurements of oil absorption by the filler.

Modulus at minimum strain essentially depends on the polymer−filler interfacial area, calculated as $A_i \times \rho \times \phi$, where A_i is the filler surface area and ρ is the filler density. Modulus at large strain mainly depends on Φc. Compounds based on fillers with large surface area have high modulus at minimum strain and remarkable reduction of modulus as the strain amplitude increases, a phenomenon known as the Payne effect [71]. Moreover, their percolation threshold in the polymer matrix is lower than for fillers with larger surface area.

As mentioned in the Introduction, most of the reinforcing fillers for rubbers used are nanostructured: CB and silica. Their aggregates have dimensions of hundreds of nanometers and can not be split into individual particles. On the contrary, the so-called nanofillers, such as clays, CNTs, graphene, and nanographites, have individual particles, with at least one dimension below one hundred nanometers, that can be individually dispersed in the rubber matrix and are characterized by a high or even very high aspect ratio. Nanofillers are thus expected to have large/very large surface area and they should promote high modulus at minimum strain. The

Table 11.2 Percolation threshold (Φ_p) of OC, CNT and nanographite in rubber matrix[a]

Nanofiller	Matrix	Φ_p (phr)	References
OC	Neat SBR	12[b]	[76]
	Neat NR	8	[77]
	Neat IR	6	[44]
	IR + 60 phr CB	3	[44]
CNT	Neat IR	7	[78]
	Neat IR	9	[25]
	IR + 60 phr CB	3	[78]
nanoG	Neat IR	21	[16]
	Neat IR	17	[25]
	IR + 60 phr CB	8	[16]

[a]The percolation threshold was calculated through the Huber-Vilgis method. Round figures are indicated in the Table.
[b]Estimated value.

mentioned nanofillers have indeed high surface area but do not have the so-called structure, that means they are not able to occlude rubber chains. Hence they are not able to transform the soft rubber into a rigid undeformable phase. In the light of these findings, nanofillers with high surface area promote a pronounced nonlinearity of the viscoelastic modulus. Nanofillers are also characterized by the low concentration in the rubber matrix required to achieve percolation. Table 11.2 reports values of percolation thresholds for nanofillers and for CB in neat rubber matrices. Such thresholds were estimated by applying to the initial modulus values a model proposed by Huber and Vilgis [75] for rubbers filled with spherical nanostructured CB. According to this model, the excess of initial modulus $(E-E_0)/E_0$ scales linearly with the filler content below the percolation threshold, whereas above this limit it increases following a power law with exponent 4. The different exponents calculated for nanofillers can be attributed to their deviation from sphericity.

Bearing in mind the overall picture, a peculiar feature of OC has to be carefully taken into account. As reported in section 11.2.3, OC are effective accelerators. The study of the mechanical reinforcement brought about by OC should always be performed bearing in mind that OC, thanks to the ammonium cations, promotes remarkable variation in the structure of the cross-link network, essentially favoring the formation of shorter sulfur bridges and higher cross-linking density. Such a variation of the crosslink network is responsible, per se, for the enhancement of the modulus of the rubber nanocomposites.

11.2.5 Dynamic-mechanical properties

In most papers, the filler networking phenomenon was investigated by applying sinusoidal stresses to nanocomposites, typically in the shear mode, increasing the strain amplitude (strain sweep test). Results reported in many papers, referring to different

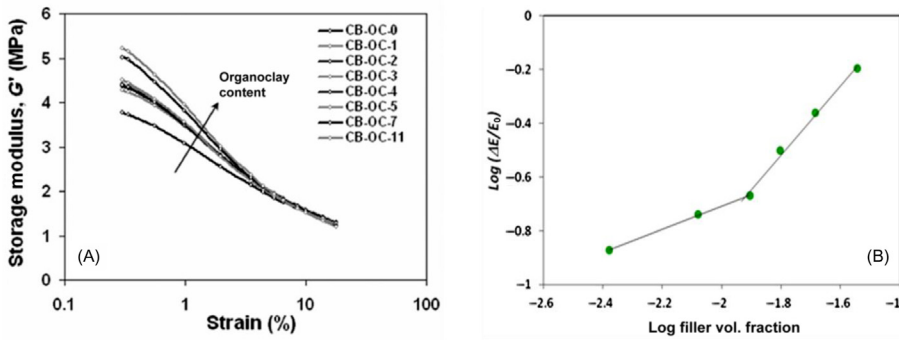

Figure 11.5 (A) Dynamic storage modulus G' in shear mode at 1 Hz versus strain amplitude for CB (60 phr)-OC hybrid composites. (B) Double logarithmic plot of the excess modulus, with respect to the matrix with 60 phr CB, as a function of the OC volume fraction (Huber-Vilgis plot).
Source: For (A) Reprinted with permission from Galimberti M, Coombs M, Cipolletti V, Riccio P, Ricco T, Pandini S, et al. Enhancement of mechanical reinforcement due to hybrid filler networking promoted by an organoclay in hydrocarbon based nanocomposites. Appl Clay Sci 2012;65−66:57−66.

rubbers, consistently agree on the remarkable increase of the Payne effect when increasing amounts of OC were added to rubber composites in the presence of CB. Data are available for OC(2HT) in SBR [41,47], in NR [24], in IR [44], for OC (ODA) in ENR [46], and for masterbatches of OC(2HT) in E-SBR, melt blended with CB and SSBR/BR [35]. In the case of nanocomposites based on NR and 50 phr of CB [42], the replacement of CB with OC(2HT, ODA) (in the same amount by mass) apparently led to the decrease of the Payne effect. However, taking into consideration the higher density of OC, also this result seems to confirm the overall picture.

It is definitely very important to carefully consider the effect of the amount of both OC and CB. In fact, in the case of the hybrid OC(2HT)/CB filler system in SBR [41], the replacement of 3 out of 45 phr of CB with 3 phr of OC led to a reduction of the Payne effect. In Fig. 11.5A, that refers to IR based composite containing 60 phr of CB, it is evident that a remarkable Payne effect occurs after a sort of threshold for the OC(2HT) content [44].

The existence of such a threshold could mean the existence of two regimes of mechanical reinforcement. An investigation was performed [44] by applying the Huber-Vilgis model to dynamic storage G' moduli at minimum strain and to initial E moduli from stress−strain curves. The double logarithmic plot of the excess of E modulus versus OC content is shown in Fig. 11.5B. Two different straight lines are in the graph of Fig. 11.5B, indicating the discontinuity in the regime of mechanical reinforcement, as if at a given OC threshold value (3 phr in the figure, lower than in the neat rubber matrix, 6 phr), OC and CB were able to form a hybrid filler system. The continuous hybrid system was visualized by TEM micrographs.

The effect of OC organization on the Payne effect of a composite based on IR and CB was studied [36]. OC(2HT) was used in its pristine state, with

stacked layers, or delaminated via ball milling. It was demonstrated that the delaminated OC brought about a much lower Payne effect, than the stacked OC. As mentioned in section 11.2.2, this result was attributed to the large volume occupied by OC stacks, that made the formation of hybrid filler networks easier. As mentioned in the same section, the affinity of OC for CB was attributed to the cation-pi interaction between the compensation ammonium and the aromatic rings of CB [22] and was reported to cause the synergistic effect by the two fillers on the mechanical reinforcement. A very low amount of the ammonium salt was needed to cause a remarkable enhancement of the composite initial modulus and of the filler networking process. In fact, maximum enhancement was estimated to occur with an ammonium salt layer, with the hydrocarbon chains lying flat on CB surface.

The storage modulus of nanocomposites was investigated from below to above the glass transition temperature (T_g).

Most results indicate that the modulus increases, below the glass transition, by adding OC to the CB based composite and such an increase depends on the type of substituents. OC(T2HE) and OC(2HT), added in 3 phr amount to SBR-based composite, to replace 5 out of 40 phr of CB, brought a clear increase of storage modulus, to different extents [40]. The same findings were obtained by adding the same OCs to an EPDM based composite, to replace 3 out 40 phr of CB [45]. In both composites, the largest increase was observed by using OC(T2HE). More subtle differences appear for composites based on XNBR, with larger values for the OC(ODA) compatibilized thanks to a low molecular-weight liquid rubber, carboxyl-terminated copolymer of butadiene and acrylonitrile [43]. An increase of modulus was observed also in NR by adding to a composite containing either 30 or 50 phr of CB an OC(2HT) "expanded" with a different amount of SA [24]. It was reported that the "expanded OC" was easily exfoliated and the increase of modulus was supposed to be the consequence of the large interaction with the composite matrix of individual lamellae. Moreover, by the use of hybrid fillers, synergistic effects were obtained on mechanical properties: with the proper filler content (10 phr SA, 30 phr CB, and 5 phr OC), CB content and rolling resistance could be reduced at the same time without a decrease of other mechanical properties with respect to 50 phr CB filled NR. It was also reported that the addition to a composite based on ENR and 20 phr of CB of 15 phr of OC(ODA) led to an increase of T_g, whereas 15 phr of OC(T2HE) led to modulus reduction [39]. As expected, the addition of 25 phr of CB to a composite based on ESBR and containing 6 phr of OC (2HT) led to a clear increase of the modulus [47].

A similar trend was observed above glass transition temperature for the composite based on ENR and OC(ODA, T2HE) [39]. Increasing amounts of OC(ODA) led to higher values of E' above glass transition temperature, in XNBR Matrix, compatibilizing OC with a low molecular-weight carboxyl-terminated copolymer of butadiene and acrylonitrile [43]. Differences between OCs (2HT, T2HE) were subtle in SBR [40] and EPDM matrices [45].

In HNBR, with either 5 or 15 phr of CB [56] and OC(ODA) either in place of the 5 CB phr or added to the 15 CB phr, the larger values of E' and the lower Tan δ values were interpreted with the strong filler−matrix interaction.

The main drawback of OC appears to be the strong reduction of the storage modulus above room temperature. The replacement of 10 out of 60 phr of CB with the same volume amount of OC(2HT) in composites based on either IR or NR led to remarkably larger E' reduction (ΔE), passing from 23°C to 70°C: from 3.3 to 4.4 in the case of NR, from 2.7 to 3.3 in the case of IR. The replacement of 5 and 10 phr out of 60 phr of CB in SBR-based compound with the same amount of OC increased $\Delta E(23^\circ - 70^\circ)$ from 7.8 to 8.6 to 10.2 [49]. It is well documented in the literature that crystalline OC show endothermic phenomena above room temperature [79,80–82].

In a composite based on NR and OC(2HT), a secondary transition evidenced in the modulus versus temperature plots of the nanocomposites above the percolation threshold of OC was observed and was attributed to a reduction in the efficiency of load transfer from matrix to clay due to the ''melting'' of onium chains at the polymer–filler interface [77].

The effect of OC on the storage modulus of rubber composites based on CB appears clear: enhancement of storage modulus and enhancement of modulus reduction as the temperature increases. Differences and discrepancies among various results could be attributed to the different organization of OC in the rubber matrix.

The effect of OC(2HT) organization on storage modulus in the plateau region was studied [36] performing multifrequency dynamic-mechanical analysis on masterbatches containing only PI, CB, OC, and 3-octanoylthio-1-propyltriethoxysilane as the silane, obtaining a master curve representation of G' as a function of frequency. Two types of OC were used: either pristine, with some layers in crystalline stacks, or delaminated (D-OC), without any (00ℓ) reflection in the XRD pattern. It was shown that the master curves of masterbatches with only CB as the filler and with CB/D-OC hybrid filler system were almost overlapped, with the system incorporating only CB revealing a shorter and steeper plateau, with higher modulus values on the high frequencies region. The masterbatch containing pristine OC stacks was clearly different: the rubbery plateau had a major extension and a lower slope, with expansion of the low frequency end of the master curve.

OC organization, in stacks or in individual lamellae, was shown to have a profound effect also on the variation of the storage modulus with the temperature. OC, as stacks or delaminated, were used in IR based composites in the presence of CB [83,84]: $\Delta E'$ of the composites, between low (0, 10, 23°C) and high (70, 100°C) temperatures was appreciably lower when D-OC was used in place of pristine stacked OC.

It could be thus commented that stacks of OC promote larger modulus enhancement and they seem to be able to give more effective filler networking via the immobilization of polymer chains. A key role is thus played by the extent of OC exfoliation, which depends on the type of low molecular mass chemicals that interact with the clay layers and on the processing conditions.

Tan delta, that means the ratio between loss and storage modulus is investigated in many papers. It is reported that variation in shape and strength of the tan δ peaks might suggest that T_g of the samples are affected by the extent of polymer–filler interaction. Actually, this should be taken much with caution. As demonstrated in

[85], tan δ in the glass-to-rubber softening region is influenced not only by the local segmental dynamics, reflected in the magnitude of the loss modulus toward lower T, but also by filler induced changes of both G' and G''. In other words, the polymer−filler interaction should be better represented by G". However, a clear effect of OC on tan δ was shown. For example, composites based on OC(ODA, T2HE) and CB that revealed the largest enhancement of E' (see above) [39], showed also the maximum broadening of tan δ peak, interpreted with the highest effectiveness of OC and CB for the enhancement of volume of polymer−OC interface. Reduction in the height of tan δ peak was observed in the case of composites based on SBR [40] and on EPDM [45] (OC with 2HT or T2HE) and was interpreted with physical and chemical adsorption of the E-SBR molecules on the filler surface. In the case of IR, NR, and E-SBR based composites with 60 phr of CB, the replacement of 10 phr of CB with the same volume fraction of OC(2HT) led to very similar tan δ at low temperatures (10 and 23°C) and higher tan δ at 70°C [49].

The effect of OC(2HT) on the dynamic-mechanical properties of the nanocomposites was investigated [35] in the light of the application as a tire tread compound. Different amounts of OC, from 5 to 20 phr, were added to a composite based on E-SBR, S-SBR and BR and 30 phr of CB. The remarkable increase of tan δ at −10 and 10°C allowed to envisage better performances on ice and wet road and the higher E' at 30°C was assumed as indication of good dry handling. However, the much higher values of E' at −20°C and of tan δ at 60°C suggested poor winter traction and worse rolling resistance.

To reduce the heat build up of composites based on SBR, 25 phr of CB and 6 phr of OC(2HT) were used in place of 40 phr of CB, achieving a good set of mechanical properties [47]. Delamination of OC(2HT) was reported to be an effective way for reducing the hysteresis of nanocomposites based on NR [83,84]. Larger exfoliation of OC(2HT) in SBR, thanks to calcium stearate as a dispersion promoter [41] led to lower heat build up.

11.2.6 Tensile properties

It is worth considering at first, nanocomposites based on traditional, large amounts of CB, at least 60 phr.

In E-SBR based composites [49] with 60 phr of CB, the replacement of CB with the same volume fraction of OC(2HT) (5 and 10 phr) led to the reduction of moduli at 100% and 300% elongation, to larger elongation and energy at break and to larger tensile strength, with more improvement of ultimate properties with 10 phr of OC. In IR and NR-based compounds with 60 phr of CB, the replacement of CB with OC(2HT) (10 phr, same volume fraction) led to very similar results but for the increase of moduli at short deformation.

OC(quaternary ammonium) addition (5, 10, 15 phr) to a compound containing comparable amounts of NR and SBR and 75 phr of CB [51] did not cause appreciable changes in the tensile strength, but led to a gradual reduction in the elongation at break, with 15% reduction for 10 phr of OC, interpreted as the compound stiffening.

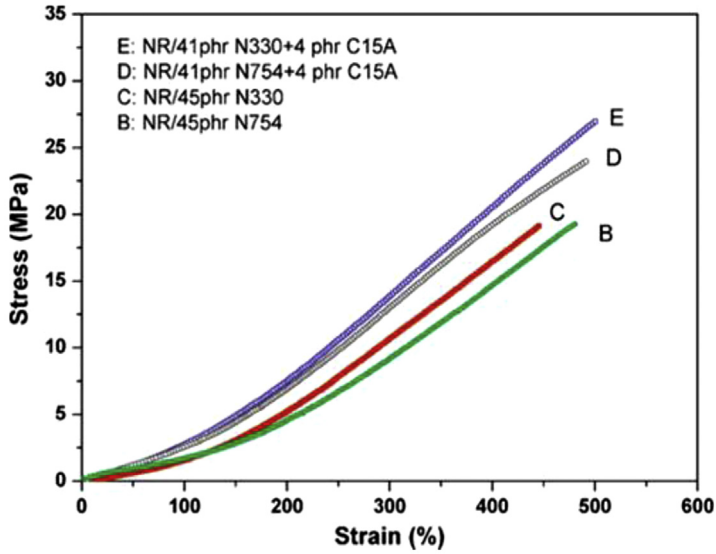

Figure 11.6 Stress−strain curves for composites based on either only CB or OC/CB filler systems.
Source: Reprinted with permission from Liu Y, Li L, Wang Q, Zhang X. Fracture properties of natural rubber filled with hybrid carbon black/nanoclay. J Polym Res 2011;18:859−67.

In the presence of a lower CB amount (45 phr), in a NR-based compound, the replacement of a minor amount of CB with OC(2HT) led to higher stresses at all elongations and better ultimate properties, as it is shown in Fig. 11.6 [48].

Again in NR matrix, modulus at 100% and tensile strength increased when 5 phr OC(2HT) were added to composites containing 20, 30, 40, and 50 phr of CB, in the presence of a slight reduction of elongation at break [24].

The replacement of CB, from 5 to 15 phr out of 50, with the same mass amount of OC (2HT, ODA) was reported to lead to a decrease of 300% elongation and tensile strength, for the highest OC contents [42]. The reinforcing effect, lower than expected, was attributed to insufficient filler dispersion.

In SBR-based composite, the replacement of 5 out 45 phr of CB with 3 phr of different OC ("HT, T2HE) led to maximum improvements of about 50% for the tensile strength and 34% for the modulus at 300%, in comparison with composites with only CB [40].

In ESBR based composites, higher EB and lower tensile strength were observed by replacing from 3 to 10 phr out of 45 phr of CB with the same mass amount of OC(2HT) [41]. It was speculated that the better clay dispersion promoted by calcium stearate helped the slippage of polymer chains on the filler surface.

The mechanical properties of EPDM filled with the OC(2HT, T2HE)-CB system were better than the properties of the EPDM−CB compound [45]. A composite

containing 6 phr of OC and 30 phr of CB showed higher moduli at 50% and 300% elongation, and better tensile strength and elongation at break than a composite containing 40 phr of CB. Better results were obtained with the OC(T2HE), which achieved the best dispersion.

Both in BIMS and in ESBR, stresses at a given strain, moduli at 50% and 100%, tensile strength, and elongation at break at a particular strain were observed to increase by adding 4 phr of OC(ODA) to composites containing either 10 or 20 phr of CB [52].

OC(ODA) was added to X-NBR based composites containing 20 phr of CB, in the range from 2.5 to 10 phr [43]. The tensile strength and the elongation at break showed a maximum at 2.5 phr as added OC. The increase of tensile stresses was not necessarily associated with a reduction of elongation at break.

Larger elongation at break and tensile strength were observed in ENR by combining 20 phr of CB and 15 phr of OC(ODA, T2HE) [39].

In NR, the combination of 20% mass of CB and OC(2HT) from 2−15% mass gave synergistic effects on tensile properties [86]. A synchrotron WAXD study proved the occurrance of strain-induced crystallization [87].

In HNBR, when 5 phr of OC(2HT) are used instead of 5 phr of CB, moduli at 50% and 100% elongation are higher but ultimate properties are, to a minor extent, worse (OC-CB-2006-Herman). Correspondingly, Shore A increases from 66 to 72. When 5 and 15 phr of OC are added to a composite containing 15 phr of CB, moduli increase at all the elongations, but elongation at break decreases.

In NR, various type of CB (in minor amounts: from 15 to 22.5 phr) were combined with a calcined clay (54 phr), not modified with an organophilic cation [88]. Hardness, 100% modulus and elongation at break were not affected by the type of CB, whereas tensile strength appreciably increased by decreasing the size of CB individual particle (N330 vs N774).

11.2.7 Tear resistance

Tear resistance was studied in composites based on a comparable amount of NR and SBR and 75 phr of CB [51]. It was unchanged up to 5 phr loading of OC(quaternary ammonium) and then became slightly lower than the reference value, with a reduction that was negligible at 10 phr and appreciable at 15 phr. It was reported that such a reduction was lower than expected, in consideration of the high stiffening effect of OC, as stiffer compounds in general show worse tear resistance. Also De Mattia crack initiation tests did not show any particular differences in the absence of in the presence of OC.

On the contrary, in the case of nanocomposites based on NR [48] and 45 phr of CB, better crack resistance was found, in the higher tearing energy region, for specimens with 4 phr of OC(2HT) in place of 4 phr of CB. It was hypothesized that either more energy dissipation occurs in the presence of the hybrid filler network or that clays promote enhanced crystallization under strains [87].

11.2.8 Abrasion resistance

The addition of OC(quaternary ammonium) (from 5 to 15 phr) to an NR-based composite containing 75 phr of CB did not lead to significant differences of abrasion resistance at the DIN (Deutsches Institut für Normung) abrader [51].

In ESBR based nanocomposites, a slight improvement of abrasion resistance was obtained by replacing 3 out of 45 phr of CB with 3 phr of OC(2HT) [41] and adopting the combination of 25 phr of CB and 6 phr of OC(2HT) in place of 40 phr of CB [47].

11.2.9 Impermeability

It is widely acknowledged that clays can promote larger impermeability of polymer composites [7,10], as permeating molecules have to go through a tortuous path. Permeability is particularly reduced if clays are largely exfoliated and are oriented perpendicular to the molecule's flow. Orientation appears a critical aspect in rubber products, such as e.g., tire compounds, that experience important dynamic-mechanical stresses.

However, the increase of impermeability of rubber products such as tire liner has great importance and large research efforts have been spent in this direction, with many patents filed on composites based on OC and CB [10]. These documents are mainly focused on the type of OC and processing conditions, but there is no indication if OC and CB have a synergistic effect on impermeability.

In the scientific literature, a recent paper on brominated poly(isobutylene-co-p-methylstyrene) (BIMS) [37] and OC(2HT) revealed that nanocomposites having both CB and organoclay had the lowest permeability, due to a synergy between the two fillers. Rubber films obtained through squeeze flow in melt compression decreased the permeability of the film, thanks to layer orientation. The key role played by exfoliation was proved. BIMS was functionalized with either triethylamine or dimethyl benzoic acid: the former chemical gave larger exfoliation and, as a consequence, lower permeability.

In NR, impermeability was observed to increase when a calcined clay (54 phr) was mixed with CB with a larger size of the individual particle: N774 was better than N550 and N330 [88].

11.2.10 Thermal stability

Ammonium cations could undergo thermal degradation in the temperature ranges experienced by rubber compounds [70,89].

It is known that alkyl ammonium salts degrade for temperatures in temperature range from 150 to 200°C [70,89], whereas imidazolinium salts are stable up to about 450−550°C. The thermal stability of nanocomposites based on EPDM was studied [45] and it was reported that compounds loaded with the hybrid OC-CB filler system had improved thermal stability. This was attributed to the heat shielding effect of the hybrid system. In particular, better stability was observed for composites with the same OC(T2HE), that gave the largest enhancement of mechanical properties.

11.2.11 Electrical properties

CR based nanocomposites loaded with CB N550 and OC(2HT) were investigated [38], determining water absorption and volume electrical resistivity, in view of the underwater application of products based on this type of rubber. The electrical resistivity requirements of rubber vulcanizates were maintained after the filler's addition.

Electrical permittivity was studied for composites based on ENR and containing CB and OC(ODA) [46]. The addition of OC led to sudden drop of relative permittivity at lower (100−100,000 Hz) and higher (100,000 Hz and 500,000 Hz) frequency ranges. However, it was surprisingly found that a composite with 20 phr of CB and 15 phr of OC(ODA) had the minimum drop of relative permittivity in both frequency ranges. This was explained with the electron tunneling through well connected network established by the so-called "nanounit". The tunneling effect was invoked to explain the electrical conductivity in nylon 6 matrix [34].

11.3 Nanocomposites based on CNT and carbon black

11.3.1 Introduction

Papers available in the scientific literature, considered for this summary, are listed in Table 11.3. Beyond the CB and CNT acronyms there is a good number of different materials, that, often, are not completely characterized (CNT in particular) in the literature. Information is lacking mainly for surface area and, in particular, activity, features that are indeed relevant for the composites' properties. It is thus interesting to analyze if it is possible to identify general behaviors, in spite, in some cases, of such a lack of information.

11.3.2 Structure

In this section, the crystalline organization of CNT, interaction of CNT with the rubber matrix, and structure of the nanocomposites are discussed, highlighting the role of CB. Studies available in the scientific literature were performed with XRD, Raman spectroscopy, TEM, SEM, and atomic force microscopy (AFM).

11.3.2.1 Crystallinity of carbon allotropes

Carbon allotropes made by sp^2 carbon atoms, such as CB, CNT, and graphite, have a common feature: they are made by graphene sheets, as it is shown in Fig. 11.7, either stacked (CB, graphite) or wrapped. One or more graphene layers are wrapped in single walled carbon nanotube (SWCNT) or multiwall carbon nanotubes (MWCNT), respectively.

In the case of CB and graphite, stacks are characterized by different number of layers, crystallinity inside the layers and shape anisotropy, that means the ratio between the crystallites dimensions in directions parallel and orthogonal to the layers [100]. In Fig. 11.8A are shown the 002 reflections of XRD patterns of CB, CNT and

Table 11.3 Papers on CNT-CB hybrid fillers: type of rubber, CB and CNT, blending technology and main aspects investigated in the work

References	Rubber	CB type	CNT type	Blending method	Analyses
[90]	NR	N330	MWCNTs (Nanocyl™ NC7000)	Melt blending by a two roll mill after solvent dispersion of CNTs	Field emission SEM, helium ion microscopy, Shore A hardness, abrasion resistance, tensile test, "edge-cut" tensile strength
[91]	SBR	CB (specific surface area 110 m^2/g)	MWCNTs	MWCNT/SBR masterbatch prepared by a coagulation process followed by melt mixing in a high shear twin screw extruder. The masterbatch was then diluted and other ingredients added by melt compounding in a Haake batch mixer	Constrained tear test, tensile test, hysteresis measurements, equilibrium swelling measurements
[23]	NR	N234; N330	Highly one-dimensional aligned multi-walled carbon nanotube bundles (CNTBs) (FloTube TM 7000)	Mechanical blending by a two roll mill	TEM, tensile test, tear test, hardness, dynamic-mechanical analysis (strain sweep in shear mode, temperature sweep in tensile mode), fracture resistance, fatigue resistance
[31]	IR, NR	N326	MWCNTs (Baytubes C150 P)	Melt blending by an internal mixer	WAXD, TEM, tensile test, dynamic-mechanical analysis (shear mode)
[92]	NR	N330; Printex XE2-B	MWCNTs (Nanocyl-7000)	Melt blending by two roll mill	Mooney viscosity, rheometric curve, Shore A hardness, tensile test, tear test, rebound resilience, compression set, dynamic-mechanical analysis (in tension mode, strain sweep), volume

(*Continued*)

Table 11.3 (Continued)

References	Rubber	CB type	CNT type	Blending method	Analyses
					resistivity, thermal conductivity, SEM
[25]	IR	N326	MWCNTs (Baytubes C150 P)	Melt blending by an internal mixer	TEM, WAXD, dynamic-mechanical analysis (in shear mode, strain sweep)
[93]	IR	N326	MWCNTs (Baytubes C150 P)	melt blending by an internal mixer	WAXD, TEM, tensile test
[19]	silicone	Printex XE2	MWCNTs	Mixing by a planetary ball mill	Rheological temperature sweep measurements, electrical resistance, tensile test, fatigue tests (for electrical resistance), pressure sensitivity tests, TEM
[78]	IR	N326	MWCNTs (Baytubes C150 P)	Melt blending by an internal mixer	Mooney viscosity, rheological temperature sweep measurements, density, TEM, tensile test, dynamic-mechanical analysis (in shear mode, strain sweep), electrical conductivity
[94]	NBR	Conductex SC ultra	MWCNTs (CM-100), acid and plasma treated	Solution blending	Tensile test, DSC, TGA
[21]	NR	N330	Hydroxyl MWCNTs	CNTs/NR masterbatch by ultrasonic assisted latex mixing process + melt blending by an open two roll mill	Tensile test, tear test, compression test, hysteresis tests, dynamic-mechanical analysis (in tensile mode, temperature sweep), SEM, swelling test for cross-link measurement, dynamic rheological tests (in shear mode, frequency sweep)

[95]	NR	N330	MWCNTs (by Sun Nanotech)	Melt blending by two roll mill	Cure characteristics, swelling, SEM, tensile test, fatigue test, TGA
[96]	S-SBR/ BR, NR, EPDM	N550	MWCNTs (Nanocyl-7000)	Dry mixing or mixing after solvent dispersion of CNTs, by internal mixer	Reflected light microscopy, TEM, tensile test, dynamic-mechanical tests (in shear mode, temperature sweep), dielectric measurements, fatigue tests, thermal diffusivity
[20]	NR	N330	Hydroxyl MWCNTs functionalized with coupling agent Si-69	Melt blending by two roll mill	Cure characteristics, swelling, SEM, tensile test, tear and compression tests, dynamic-mechanical analysis (in tensile mode, temperature sweep)
[97]	NR	N375	MWCNTs (Nanocyl-7000)	Melt blending by an internal mixer	Mooney viscosity, curve kinetics, tensile test, hardness, heat buildup, dynamic-mechanical analysis (in tensile mode, temperature sweep)
[98]	SBR	N330	MWCNTs (by Nanocyl)	Solution blending	TEM, electrical volume resistivity
[99]	SBR (25% styrene)	N330; Ensaco 250 G	MWCNTs (by Arkema)	Solution blending	TEM, AFM, tensile test, Raman spectroscopy, TGA, electrical resistivity

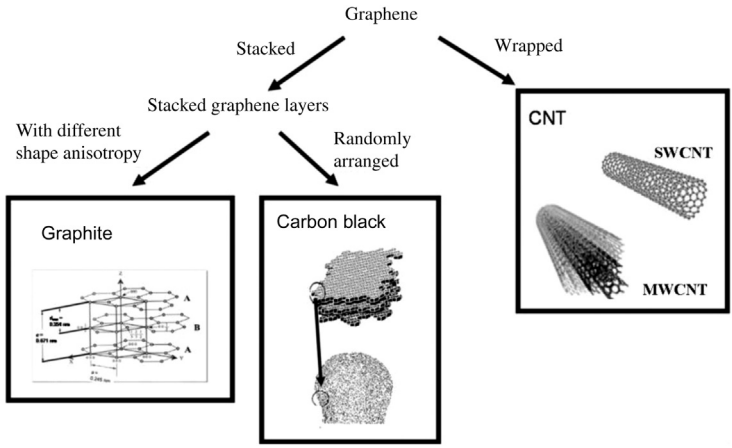

Figure 11.7 Layered structure as the common feature of carbon allotropes with sp^2 carbon atoms.

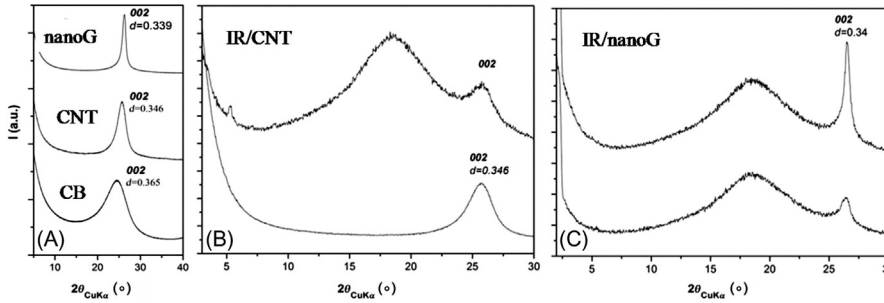

Figure 11.8 XRD patterns of carbon allotropes (A) and of IR based nanocomposites with CNT (B) and nanoG (C), uncrosslinked (lower curves) and crosslinked (upper curves). *Source*: From Galimberti M, Cipolletti V, Musto S, Cioppa S, Peli G, Mauro M, et al. Recent advancements in rubber nanocomposites. Rubber Chem Technol 2014;87(3):417–42.

nanoG [100]. As reported in [100], through the peak analysis it is possible to estimate the number of stacked layers, i.e., about 5, 10, and 35 for CB, CNT, and nanoG, respectively, reported in the figure. In the case of CNT, this number is an indication of the average number of wrapped graphene layers. In Fig. 11.8B and Fig. 11.8C, are the reported XRD patterns of nanocomposites based on IR as the rubber and either CNT or nanoG, respectively. It was calculated [31] that a higher number of wrapped layers are in the cross-linked nanocomposites rather than in the uncross-linked ones. This finding, which is quite surprising, suggests that the energy given to the compound in the vulcanization step brings a higher degree of order in CNT. The same result was obtained by taking XRD analysis on nanocomposites containing CNT and CB [78].

11.3.2.2 Interaction of CNT with the rubber matrix

Raman spectroscopy has been adopted to investigate the interaction between the polymer matrix and CNT. Nanocomposites have been prepared with CNT and SBR as the rubber [99]. In the reported Raman spectra, the G peak, characteristic of bulk crystalline graphite (graphene), shifted to higher frequencies, when CB particles or nanotubes were incorporated into the elastomeric matrix. In the case of MWNTs, the shift to higher frequencies was explained by a disentanglement of the CNTs and a subsequent dispersion in the polymer as a consequence of polymer penetration into the bundles during solution mixing. Addition of CB led to further upshifting of the G band and it was reported that better dispersion of CNT was obtained thanks to the dual phase.

11.3.2.3 Distribution and dispersion of carbon allotropes

In a nutshell, reports available in the literature clearly show the difficulty of distributing and dispersing CNT. However, they also show that CB aids CNT deagglomeration and that, upon achieving uniform distribution and dispersion of CNT, a hybrid filler network is formed.

Very poor dispersion of MWCNT was observed in SEM fracture images of nanocomposites based on NR, prepared via melt blending and containing CB (N330, total CB + CNT content equal to 25 phr); CNT (3 phr) were agglomerated into bundles. However, bundles were not observed by modifying CNT with sylane (3-triethoxysilylpropyl)-tetrasulfide (TESPT) [20].

SEM analysis of nanocomposites based on NR, prepared via melt blending and containing CB and MWCNT (N330, total amount of CB + CNT = 30 phr) revealed that acceptable fillers dispersion was obtained only for CNT content equal to 0.5, whereas it worsened by increasing the CNT amount [95].

For nanocomposites based on NR and CB (N330, 40 phr), prepared via melt blending, SEM analysis revealed that MWCNT (up to 4 phr) were not well distributed throughout the rubber matrix but were gathered in small areas [92]. CNT caused however considerable increase of CB dispersion.

The effect of mixing technology was shown for nanocomposites based on NR and containing CB (N330, up to 25 phr) and MWCNT (up to 7 phr) [21]. When only a two roll mill was used, SEM pictures revealed some agglomerates of CNT. Still some agglomerates were observed by dispersing CNT in latex. Uniform dispersion was achieved by using ultrasonically assisted dispersion of CNT in latex.

FE-SEM of composites based on NR prepared via melt blending after solvent dispersion of CNTs revealed MWCNT agglomerates, in the absence of CB, for CNT loading more than 2 phr, with the size of agglomerates increasing with CNT amount [90]. However, in the presence of CB (N330, 30 phr), large agglomerates of CB and CNT were not observed and this was attributed to the higher mixing shear.

As mentioned above, a good dispersion of CNT was obtained thanks to the mixing with CB and a hybrid filler network was formed. The simultaneous incorporation of CB (N330, 5 phr) and MWCNT in SBR, via solution blending, substantially reduced the size of CNT bundles observed by TEM analysis in

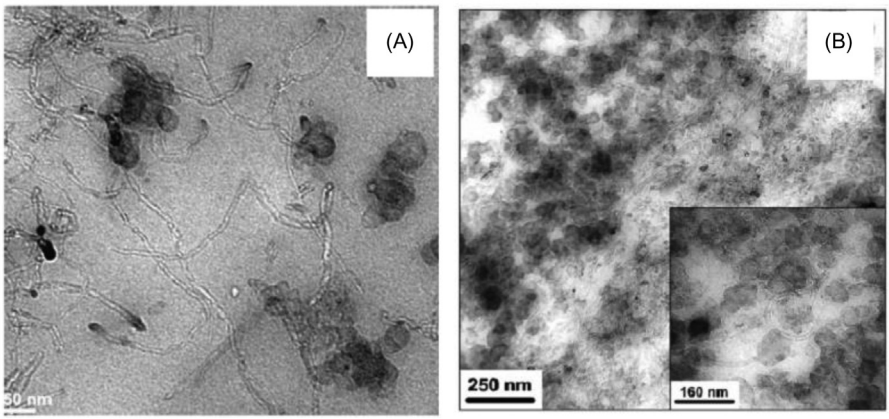

Figure 11.9 TEM images of composites containing a hybrid filler system: (A) SBR with 5 phr CB + 5 phr MWCNT ; (B) NR filled with 5.7 phr CNT and 60 phr CB.
Source: For (A) Reprinted with permission from Bokobza L, Rahmani M, Belin C, Bruneel JL, El Bounia NE. Blends of carbon blacks and multiwall carbon nanotubes as reinforcing fillers for hydrocarbon rubbers. J Polym Sci Part B Polym Phys 2008;46:1939−51. For (B) Reprinted with permission from Galimberti M, Coombs M, Riccio P, Riccò T, Passera S, Pandini S, et al. The role of CNTs in promoting hybrid filler networking and synergism with carbon black in the mechanical behavior of filled polyisoprene. Macromol Mater Eng 2013;298:241−51.

nanocomposites with only CNT. As it is shown in Fig. 11.9A, individual CNT are attached at the surface of CB aggregates [98,99]. The dual filling CB/CNT system exhibited in AFM images [99] a less rougher surface, suggesting a more homogeneous distribution of both fillers.

CNT/CB filler networks were observed in TEM micrographs and for the first time defined as hybrid filler networks [78] in nanocomposites prepared via melt blending, based on IR and CB (N326, 60 phr) and containing MWCNT in a range from 0 to 15 phr. A threshold for the CNT content was identified for the formation of the hybrid filler networks. As it is possible to see in Fig. 11.9B, above such threshold CNT webs and isolated tubes are within and inside CB aggregates and CB particles can be observed inside CNT webs, suggesting a strong CB/CNT interaction. As reported in the inset of Fig. 11.9B, CNT are also wrapped around CB aggregates and are bridges among CB agglomerates [31,93]. A continuous hybrid CNT-CB network was clearly visible in IR based nanocomposites containing the same amount of CB (N326 and MWCNT (15 phr). It was reported that the high aspect ratio of CNT tubes and their ability to wrap around CB aggregates appear to play a key role in creating the hybrid network [25].

TEM analysis of nanocomposites prepared via mixing by a planetary ball mill, based on silicone rubber, containing CB (Printex, 2.5 phr) and MWCNT (1 phr), revealed that CB particles linked the gaps between the unconnected CNT, resulting in the formation of conducting networks [19].

A rather homogeneous distribution of MWCNT (up to 5 phr) was obtained in NR-based nanocomposites having a constant hardness, prepared via melt blending, in the presence of CB (CB N234, up to 25 phr) [23]. TEM images showed that the CB aggregates were bridged by highly one-dimensional aligned CNT to form a hybrid filler network.

11.3.3 Rheology

The addition of CNT to composites containing CB leads to an increase of viscosity. The data reported in this section have arisen from composites based on NR. For composites containing 40 phr of CB (N330) [92], the increase of viscosity due to MWCNT addition was larger than that due to CB addition for amounts of added filler larger than 2 phr; for 4 phr filler addition, Mooney viscosity (ML $(1 + 4)100^{\circ}C$) was about 60 in the case of CNT and about 50 in the case of CB. This was attributed to the high aspect ratio of CNT, that favors the entanglement and, in turns, flow restriction. The role of shape factor of CNT in enhancing the viscosity of CB/CNT composites was highlighted also in [97] and it was reported that the value of shape factor was not constant, passing from about 53 to about 34 for CNT content from 2.5 to 15 phr. The shape factor was evaluated by fitting the Einstein-Guth equation [74] to experimental results of Mooney viscosity.

The effect of shear rate on complex viscosity was studied [21] and results were correlated with the occurrence of the percolation network. For composites based only on CNT, it was seen that the complex viscosity increased with the loading level of CNT and the shear viscosity decreased with an increase in the shear rate. In the region of low frequencies, a pseudoplastic shear thinning behavior appeared (Newtonian plateau disappeared) by increasing the CNT content and this was attributed to the formation of a percolated CNT network. For CB/MWCNT composites (CB N330, 25 phr as total amount of filler) high shear thinning behavior was clearly observed.

11.3.4 Curing

In the literature, information is available on cross-linking of rubber nanocomposites, containing CB and CNT, promoted by either peroxide or sulfur based systems. As mentioned previously, the surface characteristics of carbon allotropes, such as surface area and activity, play a fundamental role, in particular in vulcanization reactions. They are not always reported in the papers on diene rubbers vulcanization. The summary reported in the following sections is thus based on the available data.

11.3.4.1 Crosslinking with peroxide

Nanocomposites containing CB and CNT in 1:1 as the mass ratio (and as volume ratio as well, as they had the same density) from 2.5 to 30 as the total filler content were cross-linked with dicumyl peroxide [31], without observing any appreciable

difference, either among the different composites with the hybrid filler system or with the composites with only one carbon allotrope. Characteristics of curing could be attributed to peroxide, a low induction time and absence of reversion.

11.3.4.2 Crosslinking with sulfur based system

As already mentioned in this Chapter, it is widely acknowledged that CB promotes faster sulfur based vulcanization reactions [65,66]. This is attributed to the enhanced heat transfer in the rubber matrix, thanks to CB. Moreover, it is reported that both the degree of cross-linking and cure rate increase with increasing surface area and sulfur content, whereas the optimum cure time and scorch time decrease [101]. In the case of CNT, SWCNT were shown to reduce the activation energy and to accelerate NR vulcanization [102]. The scorch time of NR vulcanization decreased with the addition of acid treated CNTs [103], without substantial effect on the optimum cure time. On the contrary, carboxylic acid groups and quinone oxygen atoms were reported [104,105] to delay NR vulcanization, as a consequence of the absorption of basic accelerator species.

Acceleration of curing was found by increasing the amount of MWCNT (from 2.5 to 15 phr) in NR-based composites containing CB (N375, from 50 to 65 phr) [97]. A consistent decrease of t_{50} and scorch time (scorch safety) measured at 127°C was observed. Such findings were commented to be unexpected and were justified with the residual amount of catalyst used for CNT synthesis.

In the case of NR/CB composites, containing CB and MWCNT (N330, total amount of CB + CNT = 30 phr) [95], the increase of CNT relative amount (CB/CNT ratio from 29.5/0.5 to 25/5) led to a consistent reduction of scorch time and curing time, as well as to the increase of the maximum M_H modulus.

Vulcanization was studied for IR/MWCNT nanocomposites containing from 1.1 to 13.3. phr of CNT, in the absence and in the presence of CB (N326, 60 phr) and the increase of the cross-linking reaction rate was observed in the presence of CB [78].

For nanocomposites based on NR and CB (N330, 40 phr) [92], scorch and curing times, minimum and maximum torque, and the torque difference were found to increase with increasing CNT content (up to 4 phr), though the dispersion of the nanotubes is not good.

In the case of composites based on NR/CB (N330, 30 phr) [90], scorch and cure times slightly decreased with increasing MWCNT content, while their torque difference (M_H-M_L), increased. The dilution effect and thermal conductivity enhancement of MWCNT were commented to be responsible for the obtained results.

Instead, in the case of NR/CB based composites (N330, total CB + CNT amount equal to 25 phr) when CNT were modified with TESPT as the silane coupling agent, the vulcanization and the scorch times increased with increasing content of CNT. These results were explained with the absorption of curing chemicals on the CNT surface [20].

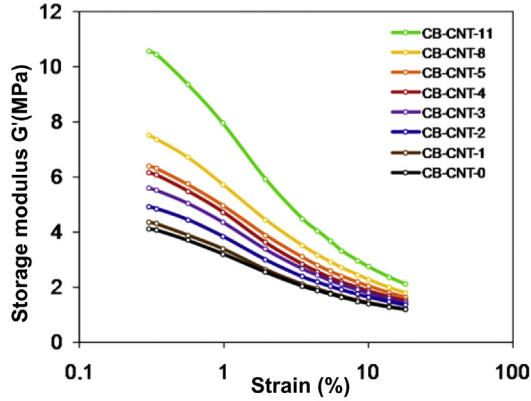

Figure 11.10 Strain dependence of storage modulus G' for CB/CNT hybrid composites. *Source*: Reprinted with permission from Galimberti M, Coombs M, Riccio P, Riccò T, Passera S, Pandini S, et al. The role of CNTs in promoting hybrid filler networking and synergism with carbon black in the mechanical behavior of filled polyisoprene. Macromol Mater Eng 2013;298:241−51.

11.3.5 Dynamic-mechanical properties

Dynamic-mechanical properties of cross-linked composites based on CNT and CB were studied by applying sinusoidal stresses both in the shear and tensile mode and cross-linking the composites both with peroxide and sulfur based systems.

From strain sweep tests, it was seen that when CNT were added to neat polymer matrix (IR), they gave rise to remarkable filler networking [31], in the presence of a cross-linking network made by short bridges such as the one formed by a peroxide. Filler networking drastically increased above the percolation threshold but was detectable also below such a threshold. In the presence of CB (N326, 60 phr) [31,78], in IR based composites cross-linked with sulfur, CNT increased the filler networking, as it is shown in Fig. 11.10, in particular above a critical concentration threshold, as in the neat IR matrix.

Interestingly, it was found that CNT increased the low amplitude storage modulus of the matrix, in the presence or in the absence of CB, by a factor depending only on its content. This aspect will be discussed more in detail, to attempt a rationalization of literature data, below in the text.

Composites based on NR and containing 25 phr as total level of carbon allotropes (CB N234, MWCNT) revealed a clear increase of filler networking when CB was replaced by the same mass amount of CNT, from a level of at least 3 phr [23]. High hysteresis was observed by replacing CB with 5 phr of CNT. To NR-based composites with 40 phr of CB (N 330), CNT was added (from 2 to 4 phr) and promoted much more filler networking than a conductive CB [92].

CNT/CB/NR nanocomposites were prepared by latex blending of CNT (containing 3% of hydroxyl groups) and NR and successive melt blending of this

masterbatch with NR and CB, keeping the total amount of filler at 25 phr with increasing amount of CNT, from 1 to 7 phr [20,21]. An increase of storage modulus, in particular above $-40^{\circ}C$, and increase of tan δ peak were observed, and reported as synergistic effects. MWCNT were shown to promote a remarkable increase of heat build up [97] when they were added to NR/CB (N375, 50 phr) composites, from 2.5 to 15 phr. It was hypothesized that the high internal friction was due to the poor interaction between the nanotubes and the polymer matrix.

11.3.6 Tensile properties

The hybrid CNT-CB filler systems are able to promote substantial improvements of modulus, tensile strength, and strain at break, with respect to composites filled with a single carbon allotrope. Data available in the literature show that the amount and the extent of dispersion of CNT are crucial to achieve improvements rather than a worsening of the mechanical properties.

SBR-based composites were prepared with CB (N330), MWCNT (5 phr), or a mixture of both fillers (CB 10 + CNT 5) [99]. With the latter composite substantial improvement of mechanical properties was obtained. Also by keeping constant the total amount of filler (10 phr), better mechanical properties, in particular ultimate properties, were obtained in the presence of the dual filler system. Values of stresses were plotted using the semiempirical Mooney-Rivlin equation (Eq. (11.3)) [106].

$$\sigma * = 2C_1 + 2C_2\alpha^{-1} \tag{11.3}$$

in which C_1 and C_2 are constants independent of α, and σ^* is the reduced stress, i.e.,

$$\sigma * = \sigma/(\alpha - \alpha^{-2}) \tag{11.4}$$

The plot shown in Fig. 11.11 reveals an upturn in the modulus at a lower extension ratio and a large increase in the reduced stress, that were correlated with the increase in the cross-linking density created by polymer−filler interactions.

On the basis of the curves in Fig. 11.11, it was commented that the presence of CB leads to a better interaction between CNT and polymer chains. It was also investigated as the Mullins effect, a hysteretic mechanism occurring during deformation of the material, that corresponds to a decrease in the number of elastically effective networks chains [107].

Stress softening was more pronounced in the sample containing the dual filler system, confirming improved interactions with polymer chains, when CB and CNT were dispersed together in the rubber matrix.

In composites based on NR and CB (N330, 30 phr) [90], the addition of CNT (from 2 to 8 phr) led to an increase of hardness and of 100% modulus. The tensile strength was not modified by the addition of CNT to CB filled NR, instead it was observed to decrease when CNT were added to the neat polymer matrix. These results were attributed to the increase of cross-linking density and to the better dispersion of CNT in the presence of CB.

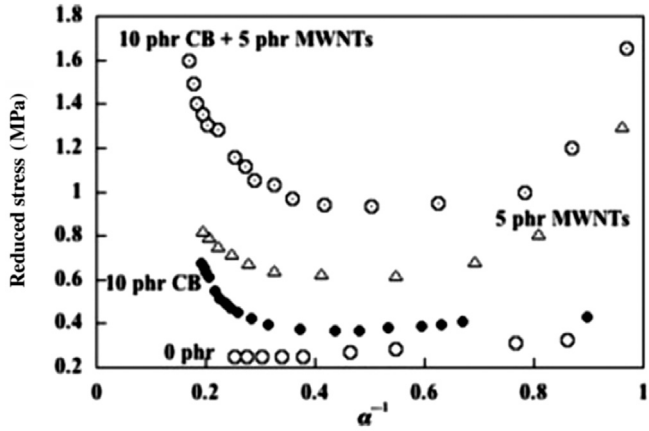

Figure 11.11 Mooney-Rivlin plots for pure SBR and for SBR composites.
Source: Reprinted with permission from Bokobza L, Rahmani M, Belin C, Bruneel JL, El Bounia NE. Blends of carbon blacks and multiwall carbon nanotubes as reinforcing fillers for hydrocarbon rubbers. J Polym Sci Part B Polym Phys 2008:46;1939−51.

Increases of tensile stress at all elongations and of tensile strength and the occurring of failure at higher stresses were observed by adding 3 phr of MWCNT to 40 phr of CB in SBR-based composites [91]. CNT were commented to act as crack bridging elements that inhibited tear propagation. This was attributed to strong surface interaction between CNT and SBR.

Nanocomposites based on NR with a fixed hardness level, obtained by partially replacing 25 phr of CB with CNT, revealed synergetic reinforcing effects: substantial increases of stresses at 100 and 300%, tensile strength, and tear strength were observed when CNT were used in place of CB (1 phr CNT for 3 phr of CB), up to 5 phr of CNT [23]. Strain-induced crystallization was also enhanced by the addition of CNT, that was hypothesized to lead to greater strain amplification near the crack tip.

Clear enhancement of stresses at all elongations was observed by adding MWCNT (from 1 to 9 phr) to IR based composites containing 60 phr of CB (N326) [31,78]. For comparison, composites with the same amount of MWCNT but without CB were prepared. These data allowed to estimate the initial modulus as the slope at the origin of stress−strain curves and to evaluate the modulus enhancement due to CNT addition with respect to the composite free of CNT (with or without CB). Such enhancement was found to depend only on the amount of CNT, irrespective of CB addition. This point is discussed below in the text, in section 11.6.

Increases of hardness, 100% modulus, and tensile strength were observed for composites based on NR and containing 25 phr as total level of carbon allotropes (CB N234 and MWCNT), when CB was replaced by the same mass amount of CNT (up to 4 phr) [92]. The higher cross-linking density and the entanglement of polymer chains with CNT were commented to be at the origin of these results.

Increases in tensile strength and strain to failure, with respect to the neat rubber matrix, were obtained by adding CB and CNT to silicone rubber [19]. Better results were achieved with 2.5 CB and 1 CNT with respect to 3 CB or 4 CNT.

The tensile strength and modulus enhancement of nanocomposites based on NBR, conductive CB (20 or 40 phr), and MWCNT treated with acid treatment or plasma (up to 9 phr) [94] gradually increased with increasing CNT content, when compared with the matrix and with the rubbers filled with the same amount of CB. In particular, the tensile strength and modulus of the composite with a CNT content of 9 phr increased up to 31% and 91%, respectively, with respect to the matrix.

In CNT/CB/NR nanocomposites, very uniform dispersion of CNT (containing 3% of hydroxyl groups) was obtained by latex blending [21] and this led to synergistic reinforcing effects. The nanocomposite (prepared by melt blending) containing 20 phr of CB and 5 phr of CNT reached the best mechanical properties: stress at 300%, tensile strength, and elongation at break. Larger amounts of CNT led to worse properties. CNT was described to bring ideal toughening and reinforcing effects, thanks to its interfacial interaction with the NR matrix.

In the case of nanocomposites based on NR, prepared via melt blending and containing MWCNT and CB (N330, total amount of CB + CNT = 30 phr) [95], the enhancement of tensile strength and elongation at break was obtained only for a low content of CNT (0.5 phr) and the decrease for larger CNT amounts was attributed to the filler−filler interaction, which was preferential with respect to the filler−polymer interaction, that favored the formation of filler agglomerates.

In EPDM as the matrix, the addition of 3 phr of MWCNT, assisted by ethanol, to 40 phr of CB (N550) led to a clear enhancement of stresses at any elongation, whereas the addition in the absence of ethanol caused a dramatic worsening of reinforcement and elongation at break [96]. This was correlated with the formation of agglomerates in the latter case.

MWCNT were added to NR/CB (N375, 50 phr) composites, from 2.5 to 15 phr [97]. It was hypothesized that the high internal friction was due to the poor interaction between the nanotubes and the polymer matrix and caused a dramatic increase of hardness and moduli and a clear reduction of elongation at break. The modulus was nearly doubled at 10 and 15 phr as the CNT content. Such a reinforcing effect was explained with the hydrodynamic effect and the Einstein-Guth equation [108] was used to calculate the shape factor of CNT, which achieved a value of about 50, one order of magnitude larger than that typical of CB.

Fig. 11.12 shows the comparison of stress−strain curves for composites based on 60 phr of CB (N326) and various added fillers, cross-linked with peroxide [31]. It appears that CNT leads to larger stress values at all strains. It is interesting to observe that an organoclay (with 2HT as the compensating cation) leads to lower reinforcement even with respect to the neat polymer matrix.

These findings indicate that CNT per se promote mechanical reinforcement, whereas OC appear to need the interaction of the compensating cation with a sulfur-based cross-linking system.

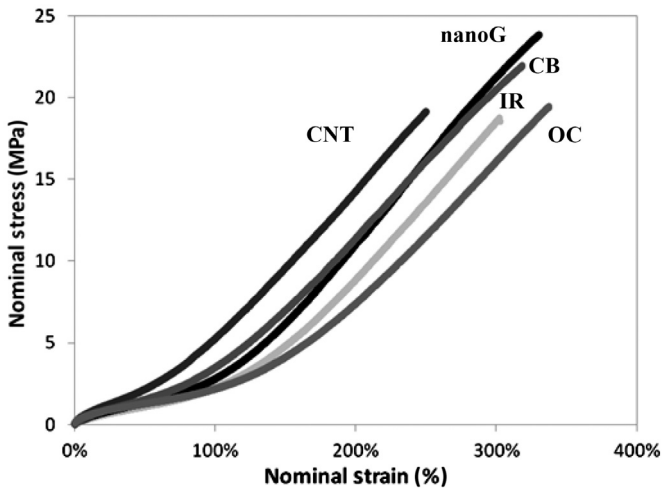

Figure 11.12 Nominal stress versus nominal strain curves for peroxide cross-linked IR based composites. The matrix is: IR + 60 phr of CB. Curves refer to composites without any added filler (IR) or containing 60 phr of CB and 12 phr of: either OC, or CNT or CB.
Source: Reprinted with permission from Galimberti M, Cipolletti V, Musto S, Cioppa S, Peli G, Mauro M, et al. Recent advancements in rubber nanocomposites. Rubber Chem Technol 2014;87(3):417−42.

11.3.7 Fracture resistance

The fracture resistance of composites based on CNT and CB was studied both under quasistatic and under cyclic (fatigue) loading. The addition of both CNT and CB was found to increase quasistatic fracture resistance, while an increase of fatigue resistance was observed only for small amounts of CNT.

The addition of 40 phr CB to a SBR matrix causes an increase in tear energy (evaluated from constrained tear test) of about 60% with respect to the near matrix, while adding both 40 phr CB and 3 phr MWCNT causes an increase of 280% [91]. The higher energy was achieved by an increase of both stress and elongation at break. This substantial improvement was attributed to a crack bridging effect exerted by CNTs during fracture propagation, to strong surface interactions between MWCNT and SBR matrix, and to the uncoiling of curved CNT during the stretching process. Hybrid filler NR-based composites were prepared by partially replacing 25 phr of CB (N234) with increasing amounts of highly one-dimensional aligned CNTs bundles (CNTBs) up to 5 phr, by keeping the composite hardness fixed [23], in order to evidence synergistic effects by the two fillers. J-integral testing on single edge notched in tension specimens showed an enhanced fracture resistance both at initiation and propagation by CNTB addition. In the same work, fatigue resistance was found to increase up to 3 phr CNTB, while higher contents of CNTB (5 phr) led to higher hysteresis, which accelerated the rupture of material under dynamic conditions, and thus decreased fatigue crack growth resistance.

MWCNT were added up to 5 phr to a CB (N330)/NR matrix [95]. The total amount of hybrid filler was fixed to 25 phr. Fatigue life of hybrid nanocomposites increased for the composite with 25.5 and 0.5 phr of CB and CNT, respectively. At higher amounts of CNT, it was hypothesized that agglomeration of CNT could be responsible for the reduced fatigue life.

11.3.8 Abrasion resistance

The abrasion resistance was found to increase by increasing MWCNT content (from 2 to 8 phr) for NR-based composites containing 30 phr of CB (N330), with respect to nanocomposites containing only CNT [90]. This was attributed to the increase in hardness and modulus and to the better dispersion of CNT, due to the presence of CB.

11.3.9 Electrical properties

The addition of MWCNT, from 2 to 10 phr, to SBR-based composites containing 10 phr of CB (N330 Cabot, or Timcal, more conductive) [99] reduced the resistivity and the percolation threshold for both CB, at a smaller CNT concentration for the more conductive CB. The interconnected filler network was formed for CNT content between 2 and 3 phr and was also formed by feeding to SBR 5 phr CNT and 5 phr CB N330 [98]. It was commented that the incorporation of CNT promoted the formation of connected structures by bridging the uncontacted CB particles, as confirmed by analysis of TEM images (see Fig. 11.9 above). A gradual increase in resistivity was obtained upon applying increased deformations and this was explained by the breakdown of the conductive networks and the orientation of CB aggregates and CNT. The filler network was not reformed upon releasing the stress, as revealed by the high resistivity values. However, new stretching led to the formation of new conductive pathways with decreases in resistivity. Much higher conductivity is obtained by adding CNT to CB rather than by increasing the CB content. This appears from results reported in Ref. [98] and in Ref. [78] for IR based composites. Fig. 11.13A,B are taken from such refs.

In Fig. 11.13B, the DC conductivity monotonously increases with CNT content and the curve does not show any discontinuity, as instead was observed for the excess of initial modulus, as mentioned above discussing the dynamic-mechanical properties.

Conductive silicone rubber was obtained by ball milling, adding 2.5 phr of CB and 1 phr of MWCNT [19]. Due to the synergistic effects, the electrical resistance was lower when hybrid fillers were used than when a single filler was used with a similar overall concentration. This was attributed to the fact that CB particles effectively link the gaps between the unconnected CNT, resulting in the formation of conducting networks. A high sensitivity of electrical resistivity

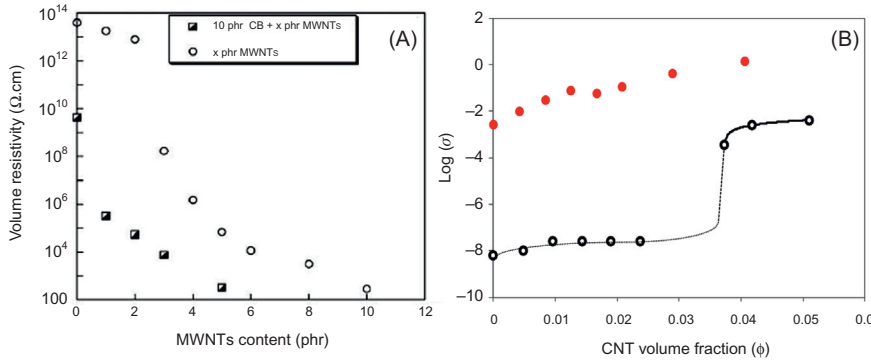

Figure 11.13 (A) Volume resistivity versus filler loading for SBR composites with 10 phr CB and CNT. (B) DC electrical conductivity versus CNT content for composites containing CNT. Composites without CB are indicated by ○ symbol in both figures.
Source: For (A) Reprinted with permission from Bokobza L. Mechanical, electrical and spectroscopic investigations of carbon nanotube-reinforced elastomers. Vib Spectrosc 2009;51:52−9. For (B) Reprinted with permission from Galimberti M, Coombs M, Riccio P, Riccò T, Passera S, Pandini S, et al. The role of CNTs in promoting hybrid filler networking and synergism with carbon black in the mechanical behavior of filled polyisoprene. Macromol Mater Eng 2013;298:241−51.

was observed to tensile and compressive stresses. However, long-term measurements revealed that excellent electrical properties were maintained after different strain histories.

Electrical percolation was obtained in NR by adding 40 phr of CB (N330). The further addition of CNT (up to 4 phr) led to a gradual reduction of the volume resistivity [92]. Also, in these nanocomposites CNT gave lower volume resistivity than CB.

11.3.10 Thermal properties

The thermal stability of nanocomposites containing CB and CNT was studied. In SBR-based composites, CB (N330, 10 phr), MWNT (5 phr), or a mixture of both fillers (10 phr CB + 5 phr CNT) appeared to have very little effect on the thermal stability of the composites [99]. A very minor effect was observed in the case of nanocomposites based on NR and containing CB (N330) and MWCNT (0.5 or 5 phr) (total amount of CB + CNT = 30 phr) [95]. A slight improvement of thermal stability was reported for composites based on NBR (35 phr), conductive CB (20, 40 phr), and MWCNT treated with acid treatment or plasma (up to 9 phr) [94]. The degradation temperature of matrix was 455°C, whereas that of the sample with 40 phr CB and 9 phr CNT was 464°C.

An increase of thermal conductivity was measured for composites based on NR and CB (N330, 40 phr) with MWCNT up to 4 phr [92].

11.4 Nanocomposites based on nanographite and carbon black

11.4.1 Introduction

Papers available in the scientific literature, considered for this summary, are listed in Table 11.4. As mentioned in the introduction in Section 11.1, graphitic nanofillers can be made by few layers of graphene and are named as nanographite, GNPs, nanosheets, or nanoflakes. Careful attention has thus to be made to the specific grade of nano-sized graphite used for the preparation of the nanocomposite.

11.4.2 Structure

Dispersion of graphitic nanofillers in the rubber matrix was remarkably increased either by blending the nanofiller with rubber latex or by using a solvent. NBR/expanded graphite (EG)/CB micro- and nanocomposites were prepared: the former by simply melt blending and the latter by latex blending EG with NBR latex, then adding CB via melt blending [113]. SEM micrographs of worn surfaces revealed, in the case of microcomposites, large graphite particles and, in the case of nanocomposites, smooth and flat surfaces because of the good graphite−rubber interfacial adhesion. The nano-size of graphite particles was crucial to avoid the formation of lubricant graphite films that reduced in microcomposites the direct contact between the matrix and the polymer. EG and modified EG (MEG) were blended (3 and 6 phr) with E-SBR (styrene = 25%) and CB (N234, 30 and 40 phr) [112]. EG was obtained from natural graphite by thermal expansion and was further oxidized with H_2SO_4/HNO_3 to prepare MEG, that contains larger numbers of polar groups on the outer surface. Delaminated EG/MEG flakes were largely prevailing in TEM micrographs when solution blending was adopted for SBR and EG, whereas agglomerates were observed in the SBR matrix when only melt blending was used.

The dispersion of graphitic layers was also much improved in the presence of CB. Hybrid nanocomposites were developed by dispersing CB (Printex XE2) and GNPs at 4−6 and 12−14 wt%, respectively, into rubbery epoxy resin [114]. CB particles improved the dispersion of GNP in the hybrid composite, as revealed by SEM analysis. In composites based on NR and CB (N330, 40 phr), a minor part of CB was replaced by the same amount of (GO) or reduced graphene oxide (RGO), from 0.5 to 5 phr [110]. TEM micrographs revealed that graphitic nanosheets were dispersed among the CB particles, as shown below in Fig. 11.14A, and that CB aggregates became smaller in the presence of nanosheets. A more developed filler network was observed in composites with rGO. However, both GO and rGO tended to aggregate at a high concentration.

Composites based on E-SBR (25% styrene), CB (10 phr) and RGO (from 1 to 3 phr), formed by in situ reduction of GO by a para-phenylene-diamine in CB/GO water suspension, were prepared by two roll milling [111]. Homogeneous

Table 11.4 Papers on graphitic nanofillers and CB hybrid fillers: type of rubber, CB, and graphitic nanofiller, blending technology, and main aspects investigated in the work

References	Rubber	CB type	Graphitic nanofiller type	Blending method	Analyses
[109]	Liquid silicone rubber	High structure CB	Graphene nanoplatelets (GNPs)	Liquid mixing method	TEM, electrical resistivity
[110]	NR	N330	Graphene oxide (GO) or reduced graphene oxide (RGO)	Solution blending	Cure characteristics, dynamic-mechanical analysis on uncured compounds (strain sweep in shear mode), TEM, tensile test, dynamic-mechanical analysis (in tensile mode, temperature sweep), Shore A hardness, swelling test, flexing resistance test (De Mattia), dynamic compression heat build-up test
[111]	Emulsion SBR		Reduced graphene oxide (RGO)	Melt blending (two roll mill)	AFM, SEM, XRD, tensile test, volume resistance test, dynamic-mechanical analysis (in tensile mode, temperature sweep), TGA
[112]	Emulsion SBR, and Oil extended carboxylated styrene butadiene	N234	Expanded graphite (EG) and modified EG (MEG)	Solution mixing or melt blending of EG and MEG + XSBR. Melt blending (two roll mill) of filled XSBR + SBR	Cure characteristics, XRD, High Resolution TEM, dynamic-mechanical analysis (in tensile mode, temperature sweep), tensile test, tear test, abrasion test,

(*Continued*)

Table 11.4 (Continued)

References	Rubber	CB type	Graphitic nanofiller type	Blending method	Analyses
	rubber (XSBR)				Shore A hardness, SEM, TGA, FT-IR
[16]	IR	N326	Nanographite (nanoG)	Melt blending	Density, TEM, XRD, tensile test, dynamic-mechanical analysis (strain sweep in shear mode)
[31]	IR	N326	Nanographite (nanoG)	Melt blending	XRD, tensile test, dynamic-mechanical analysis (strain sweep in shear mode)
[113]	NBR	N330	Expanded graphite (EG)	Melt blending (two roll mill) or latex compounding	Cure characteristics, tensile test, dynamic-mechanical analysis (in tensile mode, temperature sweep), Shore A hardness, wear test, SEM
[114]	Rubbery epoxy resin	Printex XE2 (with or without silane functionalization)	Graphite nanoparticles (GNPs) (with or without silane functionalization)	Conventional mechanical mixing (MM) or dual asymmetric centrifuge mixing by speed mixer (SM)	Viscosity test, FE-SEM, thermal conductivity, electrical conductivity, compression test

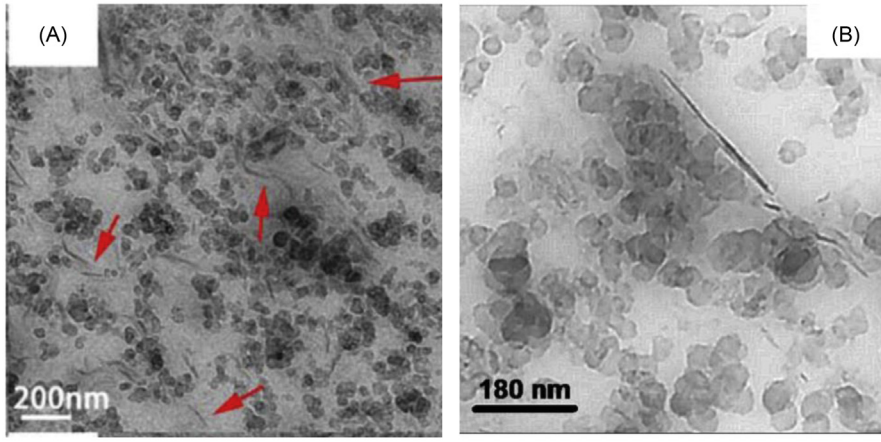

Figure 11.14 TEM micrographs of nanocomposites with: (A) 10 phr CB and 1 phr RGO; (B) 60 phr CB and 12 phr of nanoG.
Source: For (A) Reprinted with permission from Yang G, Liao Z, Yang Z, Tang Z, Guo B, Effects of substitution for carbon black with graphene oxide or graphene on the morphology and performance of natural rubber/carbon black composites. J Appl Polym Sci 2015;132 (15):41832. For (B) Reprinted with permission from Galimberti M, Kumar V, Coombs M, Cipolletti V, Agnelli S, Pandini S, et al. Filler networking of a nanographite with a high shape anisotropy and synergism with carbon black in poli(1,4-cis-isoprene) based nanocomposites. Rubber Chem Technol 2014;87(2):197−218.

dispersion of graphene sheets in SBR matrix was observed thanks to the hybrid filler system: small CB agglomerates were adsorbed on graphene surfaces. CB acted as a barrier preventing the RGO sheets from restacking.

Nanocomposites based on IR, CB (N326, 60 phr) and a nano-sized graphite with very high surface area (300 m^2/g) and high shape anisotropy, defined as the ratio between the crystallite dimensions in directions orthogonal and parallel to structural layers, were prepared via melt blending [16,31]. Even nanoG distribution with nanoG aggregates made by few-layers nanoG can be observed in Fig. 11.14B. NanoG layers are preferentially close to CB agglomerates.

11.4.2.1 Crystalline organization of G in G/CB nanocomposites

Results reported in the scientific literature demonstrate that the crystalline organization of graphitic fillers is not affected by blending with rubber matrices, both in the absence and in the presence of CB.

EG and MEG revealed larger interlayer distances between the graphene sheets with respect to pristine graphite [112]. The stacking order was retained in SBR-based nanocomposites.

When RGO (from 1 to 3 phr) was blended with CB (10 phr) and E-SBR (25% styrene) [111], composites with 2 and 3 phr content of RGO showed in XRD pattern (001) peak at the same 2θ value as in the pattern of pristine GO.

As mentioned above, when nano-sized graphite was blended with IR and CB (N326, 60 phr), the interlayer distance in graphite stacks was not modified [16,31]. The number of layers stacked in the crystalline domain increases upon applying pressure (during vulcanization) on the nanocomposite.

11.4.3 Rheology

The addition of GNP to rubbery epoxy resin, both in the absence and in the presence of CB, brought about a remarkable increase of viscosity, that was clearly dependent on the shear rate [114]. Reduction of viscosity was obtained by modification of GNP with 3-aminopropyltriethoxysilane.

Minimum torque (ML) in rheometric curves was increased by the addition of EG or MEG (3 and 6 phr) to E-SBR (styrene = 25%)/CB (N234, 30 and 40 phr) composites [112].

11.4.4 Curing

Graphitic nanofillers affect the course of sulfur-based vulcanization like the other carbon allotropes: they promote a faster vulcanization reaction. However, a key role is played by the chemical nature of their surface: the presence of polar groups can reverse this behavior.

Both scorch and optimum time of vulcanization were clearly reduced by adding to IR (in the absence of CB) increasing amount of nanographite [16]. An increase, even though less evident, was observed also in the presence of CB.

EG and MEG (3 and 6 phr) promoted reduction of scorch and optimum cure time when added to neat E-SBR (styrene = 25%) or to the E-SBR blend with CB (N234, 30 and 40 phr) [112].

On the contrary, a retarding effect on curing was observed by replacing CB (N330, 40 phr) with the same amount of GO (from 0.5 to 5 phr) [110]. This was attributed to the interaction of oxygenated polar groups on the GO surface with vulcanizers. Replacement of CB with RGO did not have any effect on scorch time but delayed the optimum time of vulcanization. This was explained with the limited diffusion of vulcanizers. At 3 phr of graphitic nanofiller, a large cross-linking density was obtained with RGO.

11.4.5 Dynamic-mechanical properties

Graphite nanofillers promote enhancement of storage modulus in the glassy region, the shift of tan δ to higher temperatures, and the increase of filler networking. A key role appears to be played by the chemical nature of the graphite surface.

The storage modulus in the glassy region of rubber nanocomposites based on SBR (E-SBR, XSBR) and CB (N234, 30 and 40 phr) was drastically enhanced by the addition of EG and MEG [112]: from about 30% (SBR/EG) to about 150% (XSBR/MEG). A substantial shift in the tan δ_{max} peak towards higher temperature was observed for EG and MEG loaded nanocomposites.

In the case of SBR (25% styrene)/CB composites, T_g shifted only slightly to higher temperature on increasing the CB amount from 10 phr to 13 phr and was found almost at the same temperature level when 1 phr of RGO was in place of 3 phr of CB. By increasing the RGO loading, T_g shifted to higher temperatures [111].

In composites based on NR and CB (N330, 40 phr), the replacement of a minor part of CB with GO (from 0.5 to 5 phr) [110] led to a remarkable increase of filler networking, as revealed by strain sweep tests performed in the shear mode. Lower nonlinearity of the storage modulus was observed by using RGO. A significant increase in flex cracking resistance was obtained with RGO, that gave much lower heat build up than GO.

11.4.6 Tensile properties

Graphite nanofillers lead to improvement of stresses at every strain when they are added to rubber composites in addition or in minor replacement of CB. The presence of polar groups on the surface can favor aggregation and, in turn, worsen mechanical properties.

In composites based on IR and CB (N326, 60 phr), the addition of nano-sized graphite (from 1 to 12 phr) [16] caused the increase of stresses at all the strains, with a progressive reduction of elongation at break.

In composites based on NR and CB (N330, 40 phr), improvement of both stress at 300% strain and tensile strength were obtained by replacing CB with a little amount of either GO or RGO (up to 2 phr) [110]. In the presence of larger amounts (up to 5 phr), improvement was observed only for stress at 300% by using RGO, whereas GO led to worsening of both static properties, as a consequence of the aggregation of GO or RGO sheets. In Mooney-Rivlin plots, the upturn of the curves, a consequence of the limitation of chain movements by neighboring fillers, occurs at smaller strains for GO content of 1 phr and RGO content of 3 phr. The upturning point increases firstly at lower CB substitution contents and then decreases gradually.

The tensile strength of rubber nanocomposites based on SBR (E-SBR, XSBR) and CB (N234, 30 and 40 phr) was appreciably increased by the addition of EG and MEG [112], from about 10% (SBR/EG) to about 150% (XSBR/MEG), whereas the increase of modulus at 300% was from about 15% to about 30% [112]. In line with these findings, hardness values were found to increase. MEG was commented to act as a better reinforcing filler (with and without CB), as a consequence of the larger interlayer spacing and the presence of polar groups on its surface. 3 phr was reported to be the optimum amount of the graphitic filler.

Tensile properties of SBR (25% styrene)/CB-RGO composites (see above for the in situ reduction of RGO) were much better compared to the SBR/CB blends [111]. For example, the moduli at 200% elongation of the SBR/CB-RG blends were higher than those of the SBR/CB blends, without reduction of elongation. The elongation at break increased from 260% to 300% when 1 phr of RGO was added to SBR/CB with 10 phr CB and the tensile strength increased by about 40% after addition of 1 phr RGO.

Compression stress−strain curve testing of rubbery epoxy resin revealed that the compressive modulus of the hybrid composites with 4 wt% CB (Printex XE2) and 14 wt% of GNP had a two-fold increase with respect to the composite with only 4 wt% CB [114]. This was attributed to the close interactions between GNPs and CB particles and to the inherent high modulus of GNPs.

11.4.7 Abrasion resistance

EG/MEG loaded SBR composites, in the presence and absence of CB, revealed lower mass loss (DIN abrasion) than composites with only CB [112].

11.4.8 Thermal and electrical properties

Thermal stability of SBR (25% styrene)/CB composites [111] was not appreciably increased by feeding RGO. With respect to composites containing RGO, the elimination of oxygenated groups from the graphitic surface was crucial.

The thermal conductivity of rubbery epoxy resin was four times improved by adding 4 wt% CB (Printex XE2) and 14 wt% of GNP [114]. Functionalization of GNP with sylane, which was reported above to reduce the compound viscosity, decreased the composite's thermal conductivity by about 15% and made the hybrid composite highly electrically insulating.

In the case of SBR (25% styrene)/CB composites, the volume resistivity was more or less the same in the presence of either 10 or 13 phr of CB (about 10^{13} Ω cm) [111]. The addition of 1 phr of RGO led to lower resistivity (about 10^{12} Ω cm), without substantial differences for a further addition of GO.

In liquid silicone rubber [109], a lower percolation threshold was found when both GNPs and CB were added to the matrix, rather than using only CB. This result was attributed to a synergetic effect of mixed GNPs and CB, indicating that the addition of GNPs increased the electrical conductivity of CB filled silicone rubber.

11.5 Nanocomposites based on CNT and silica

11.5.1 Introduction

Only a few works are available in the literature on silica−CNT hybrid filler rubber composites. They are shown in Table 11.5. Although the limited number of works does not provide sufficient data for the generalization of results, the properties obtained with hybrid fillers are briefly summarized in the following paragraphs.

11.5.2 Structure

A good dispersion of CNTs was achieved by melt blending technology for systems with a high amount of silica. Up to 3 phr of CNTs were successfully dispersed

Table 11.5 Papers on nanocomposites based on silica and CNT hybrid fillers: type of rubber, silica, CNT, blending technology, and main aspects investigated in the work

References	Rubber	Silica type	CNT type	Blending method	Analyses
[115]	SBR	Silica (Oriental Silicas Corporation, Tokusil 255) + coupling agent TESPT	Three kinds of MWCNTs with different length (M85 by Carbon Nanomaterial Technology Co., Ltd.; CM-150 and CM-250 by Hanwha Nanotech Co.)	Melt blending	Mooney viscosity, cure characteristics, tensile test, dynamic-mechanical analysis (in tensile mode, temperature and strain sweep), SEM, swelling test for cross-link measurement, heat build up, abrasion resistance, electrical impedance
[116]	NR	Highly dispersible nanoscale silica (Ultrasil 7000 GR, Evonik Degussa), silanized by TESPT	MWCNTs (Nanocyl-7000)	Melt blending	Light microscopy, TEM, dielectric analyses, tensile test, dynamic-mechanical analysis (in torsion mode, temperature and strain sweep), fatigue tests
[96]	BR/SBR, NR, EPDM	Silica Ultrasil GR 7000, Evonik + organo-silane Si 69	MWCNTs (Nanocyl-7000)	Dry mixing or mixing after solvent dispersion of CNTs, by internal mixer	Reflected light microscopy, TEM, tensile test, dynamic-mechanical tests (in shear mode, temperature sweep), dielectric measurements, fatigue tests, thermal diffusivity

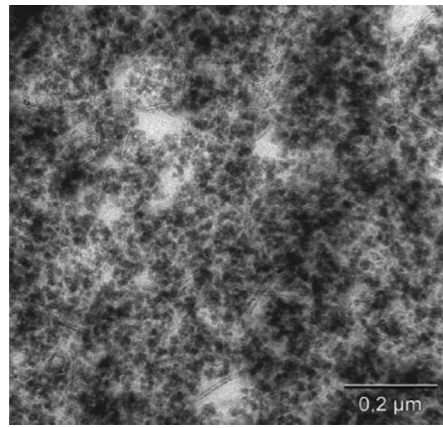

Figure 11.15 TEM image of NR filled with 6 phr CNT and 84 phr silica.
Source: Reprinted with permission from Fritzsche J, Lorenz H, Klueppel M. CNT based elastomer-hybrid-nanocomposites with promising mechanical and electrical properties. Macromol Mater Eng 2009;294:551–60.

within SBR with 80 phr silica in Ref. [115], but bundles of CNTs were observed by SEM analysis for higher amounts. In [116] no agglomeration of nanotubes was observed by TEM analysis, up to 10 phr of CNTs added to OSC/NR composites, for a total filler amount of 90 phr (Fig. 11.15).

The interaction between SBR matrix and CNTs was investigated by swelling measurements [115], but, since the formation of any chemical bonds was excluded, the reduced degree of swelling was interpreted as an increase of apparent cross-linking density.

11.5.3 Rheology and curing

It was reported that the addition of MWCNTs by melt blending reduced the vulcanization time. The cure time evaluated by t_{90} with a vulcameter was reduced by 3 phr MWCNTs added to a SBR/BR composite by dry mixing, and this result was attributed to the huge specific surface area of the CNT [96]. When up to 7 phr were added in a SBR matrix filled with 80 phr silica [115] CNTs definitely increased the cure rates due to enhanced thermal conduction, and considerably increased the Mooney viscosity due to the hydrodynamic reinforcement. The high aspect ratio and large interfacial area of CNTs were commented to be the reason for a restriction in the matrix fluidity and therefore for a viscosity increase.

11.5.4 Dynamic-mechanical properties

Dynamic-mechanical measurements were performed on hybrid filler silica–CNT systems with a high amount of silica. Dynamic moduli were obtained both in

temperature sweep and in strain sweep, to study the Payne effect. Generally, CNT addition reduced the loss factor peak at the glass transition temperature and increased the Payne effect.

Dynamic-mechanical tests were performed in tensile mode to evaluate dynamic properties related to tire performance in SBR composites filled with 80 phr silica and up to 7 phr MWCNTs [115], obtained by melt blending. Three different kinds of CNT with different lengths were used. The Payne effect was found to be increased by increasing CNT content, but only when using longer CNTs (30 and 100 μm long), while shorter CNTs (5 μm long) did not cause any remarkable effect (Fig. 11.16). Adverse effects of longer CNT addition above 4 phr were recorded also for other dynamic properties: frictional hysteresis increased, loss factor at 0°C (related to wet traction) decreased, and loss factor at 70°C (related to rolling resistance) increased. On the contrary, the addition of short CNTs with low loading enhanced the wet traction of the silica/SBR composite. The influence of longer CNTs was attributed to a scarce dispersion of CNTs, which resulted in the segregation of silica particles and aggregation of CNTs. It was commented that both the amounts of the fillers and the length of CNTs should be considered as parameters influencing the mechanical properties of SBR compounds.

Dynamic-mechanical properties were measured also for NR-based composites with a fixed total amount of hybrid filler (silica + MWCNTs up to 10 phr), obtained by melt blending [116]. Dynamic moduli measured during temperature sweeps

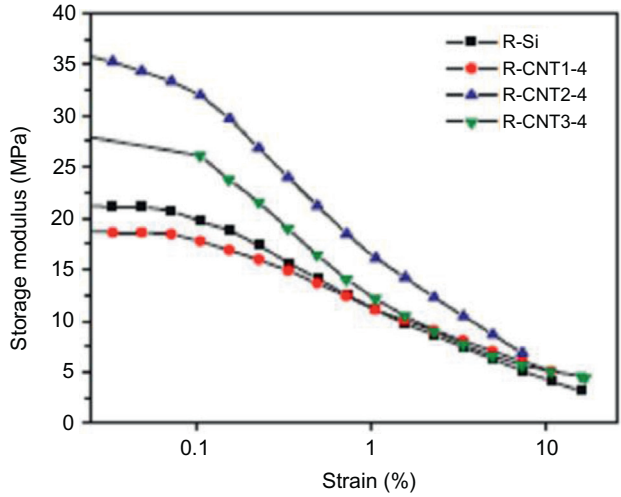

Figure 11.16 The Payne effect of SBR composites filled with 80 phr silica and up to 7 phr MWCNTs of different lengths (CNT1: 5 μm, CNT2: 30 μm; CNT3: 100 μm).
Source: Reprinted with permission form Park SM, Lim YW, Kim CH, Kim DJ, Moon WJ, Kim JH, et al. Effect of carbon nanotubes with different lengths on mechanical and electrical properties of silica-filled styrene butadiene rubber compounds. J Ind Eng Chem 2013;19:712−19.

revealed that the increase of CNT content reduced the peak of loss factor at the glass transition temperature: this was commented to be an effect of the polymer−filler interface, increasing with the nanofiller amount. The Payne effect was increased by the addition of CNTs, particularly at the highest CNT content (10 phr) and this effect was attributed to the formation of bound or trapped rubber with CNT.

11.5.5 Tensile properties

Papers show common effects of CNT addition on tensile properties, independently of the matrix considered: CNT increase stresses in the tensile stress−strain curve, while elongation at break is negatively affected after a certain CNT loading, depending on the composite considered.

A clear increase of 300% modulus was obtained by the addition to a SBR matrix filled with 80 phr silica with three kinds of MWCNTs (up to 7 phr) of different lengths (5, 30, and 100 μm) [115]. This effect was explained by the hydrodynamic effect. Tensile strength was not clearly affected by the CNTs presence, while elongation at break was reduced when increasing the nanofiller content, already at 1 phr CNT.

The stress values of stress−strain curves were increased by MWCNTs content also in composites based on NR and filled with a total amount of 90 phr of silica + MWCNTs (up to 10 phr) [116]. The elongation at break did not decrease by the addition of CNTs up to 6 phr. At higher CNT content the detrimental effect on elongation at break was attributed to the presence of agglomerates which behave as stress concentrators (Fig. 11.17).

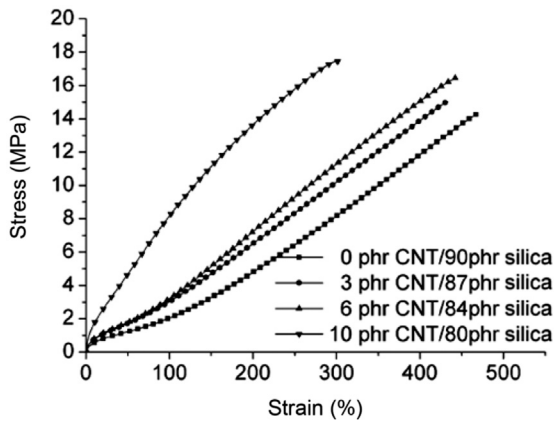

Figure 11.17 Quasistatic stress−strain behavior of composites with varying amounts of silica and CNT.
Source: Reprinted with permission from Fritzsche J, Lorenz H, Klueppel M. CNT based elastomer-hybrid-nanocomposites with promising mechanical and electrical properties. Macromol Mater Eng 2009;294:551−60.

Similar results were obtained by adding 3 phr MWCNTs either to a silica filled SBR/BR or to a silica filled NR (silica content: 40 or 60 phr) [96]. For both matrices, mechanical stresses were increased, while failure strains decreased by CNT addition. In the case of SBR/BR-based composites, an insufficient filler−polymer interaction was invoked.

11.5.6 Fracture resistance

Fatigue resistance was investigated by dynamic fracture mechanical investigations, performed on notched strip samples in tension mode.

The partial replacement of 90 phr silica with MWCNTs (up to 10 phr) in NR matrix led to the increase of the crack propagation rate [116] with respect to the silica filled NR. This effect was larger at higher tearing energies, corresponding to higher elongations, in agreement with a decrease in elongation at break by CNT addition.

Qualitatively similar results were obtained from the comparison of fatigue resistance of NR + 3 phr MWCNTs with or without 40 phr silica in Ref. [96].

11.5.7 Abrasion

Abrasion properties of hybrid filled CNT−silica composites were presented only in Ref. [115]. An SBR matrix was added with 80 phr silica and 1 to 10 phr MWCNTs of three different lengths. Abrasion resistance was measured by a Lambourn abrasion tester (Ueshima) according to ISO 23794. The addition of MWCNTs led to a decrease of abrasion resistance and an increase of heat generation at repeated dynamic impacts (measured by a Goodrich flexometer). This result was related to the decrease of elongation at break and the increase of the irreversible deformation by the CNT addition.

11.5.8 Electrical properties

The effect on electrical conductivity of the addition of 1 to 7 phr of three different MWCNT with different length to SBR filled with 80 phr was studied in Ref. [115]. The higher the MWCNT length (5, 30, and 100 μm) then the lower the amount of CNTs necessary to achieve the electrical percolation threshold (4, 2, and 2 phr, respectively). This effect was attributed to the higher effectiveness of longer lengths, which allow to achieve more easy connection points between them.

The conductivity was also significantly increased with the amount of CNT in NR filled with 90 phr of silica + MWCNT (1 to 10 phr) [116]. The percolation threshold was found below 0.6 vol% MWCNTs (equal to about 3 phr) and this indicated a quite good dispersion of the nanofiller. By the measurement of dielectric properties as a function of frequency, and by an interpretation of results based on the percolation theory, further insights into the qualitative properties of conduction mechanism in CNT/polymer composites are given. The conduction mechanism found was the same proposed for CB filled composites. The characteristic

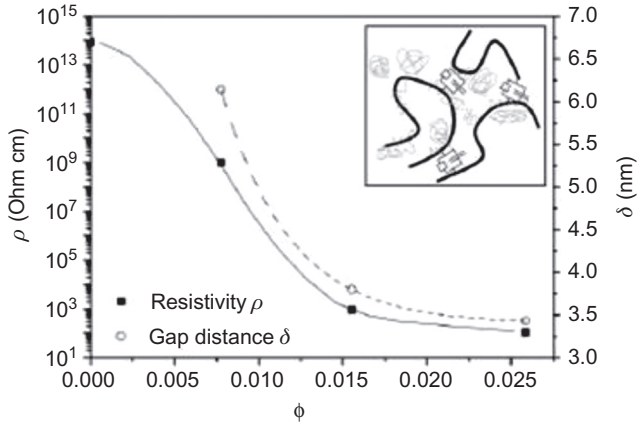

Figure 11.18 DC resistivity and distance between CNT as a function of CNT volume fraction.
Source: Reprinted with permission from Fritzsche J, Lorenz H, Klueppel M. CNT based elastomer-hybrid-nanocomposites with promising mechanical and electrical properties. Macromol Mater Eng 2009;294:551–60.

frequency of the relaxation transition observed at high frequencies can be related to the distance between adjacent filler particles. Fig. 11.18 shows that the gap distance between nanotubes exponentially decreases with the increase in CNT content and does reach a plateau value. Moreover, the decrease in gap distance is related to a decrease in resistivity. This indicates that adjacent tubes are not in direct contact, but are separated by thin polymer layers which hinder the charge transport.

The presence of silica in CNT filled SRB/BR or NR seems to increase electrical conductivity: for SBR/BR, the addition with 3 phr MWCNTs gave an electrical conductivity of 0.10 S/m, which was increased to 0.15 S/m by further addition of 40 phr silica [96]. Silica was commented to help dispersion of the CNT and accordingly, to lower the percolation threshold. A higher amount of silica (60 phr) led to lower conductivity, probably due to lower CNT volume fraction. A similar effect of the presence of both silica and CNTs was found in NR matrix, but the conductivity values were significantly lower than for SBR/BR matrix, possibly due to the different CNT blending technique ("drying mixing" for NR, mixing with ethanol for SBR/BR).

11.6 Rationalization of the mechanical reinforcement

As shown in previous paragraphs, a good number of reports are available on rubber composites with hybrid filler systems. However, they are characterized by a large variety of preparation method, type of ingredients, filler amount, degree of filler dispersion, and properties explored. Therefore, it appears difficult to attempt a rationalization. However, limiting the attention only to mechanical reinforcement, a

contribution to rationalization was given by the authors of this chapter. By analyzing the increase of the initial modulus, the synergistic effect between different fillers was pointed out and a key for the interpretation was proposed.

Mechanical reinforcement effects promoted by a single filler in a rubber matrix have been widely explored in the literature. Brief comments were proposed in section 11.2.4. Rigid particles embedded in a soft, elastomeric matrix increase the material stiffness. Literature works analyzed the dependence of stiffness on filler content, and Huber and Vilgis [75] identified the presence of at least two regimes: by plotting the modulus increase versus the filler volume fraction on a double logarithmic plot, at low filler content the modulus increases by a linear law, at high filler content the modulus increases by a steeper linear law. The filler content at which the change of regime occurs is related to the mechanical percolation threshold (Φ_c). Above the percolation threshold, the distance among filler particles decreases and a sort of continuous network occurs, which allows the filler to be more effective toward the reinforcement.

The authors have measured the percolation threshold by the Huber-Vilgis plot for single nanofiller systems. Surprisingly, also when the nanofillers were added with 60 phr of CB N326 to the same matrix a discontinuity of the modulus−filler content plot could be observed, and a pseudopercolation threshold measured. The pseudo-threshold value was lower than that found for single-filler systems, as if the nanofiller was able to establish, with CB, a continuous hybrid network, which was shown by TEM analyses. As it was shown in Table 11.2, the percolation threshold of CNT in IR was reduced from 7 to 3 phr by the addition of CB [78], that of OC in IR from 6 to 3 phr [44], and that of nanoG in IR from 21 to 18 phr [16]. This result pointed out that CB favored the dispersion of the nanofiller and the formation of a continuous hybrid filler network, which is more efficient that the one based on a single filler.

With the aim to study the strength of interaction of nano- and nanostructured fillers, in a first approach the authors analyzed composites prepared by adding various amounts of nanofillers (either OC, CNT, or nanoG) to a neat IR matrix or to composites based on IR and 60 phr of CB [16,44,78]. The strength of interaction between nanofiller and CB particles in the hybrid filler systems was quantified by comparing the measured moduli of the hybrid systems with those computed by a simple additive rule, indicated as the "additive model" [117]. Such a rule was first proposed to study the influence of the mutual interaction of two different fillers on the mechanical reinforcement of an elastomeric matrix.

The additive model provides moduli values calculated under the hypothesis that no interaction occurs between two different fillers, therefore the measurement of experimental values higher than the calculated ones can indicate an interaction between the two fillers. The predicted moduli, $E(\Phi_{CB},\Phi_{nanofiller})$ for CB and a nanofiller, are obtained as the sum of different contributions: the matrix modulus and the modulus enhancements independently originated by each single filler with respect to the neat matrix, for a given filler content. $E(\Phi_{CB},\Phi_{nanofiller})$ is calculated by the Eq. (11.5) (also referred to as "additive model"):

$$E(\Phi_{CB},\Phi_{nanofiller}),=E(\Phi_{CB})+E(\Phi_{nanonanofiller})-E(IR) \tag{11.5}$$

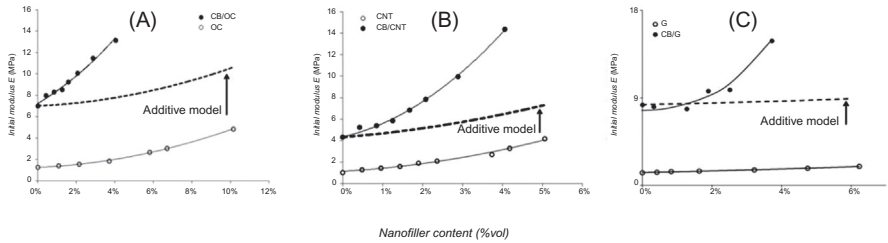

Figure 11.19 *E* initial modulus values for nanocomposites containing: (A) OC; (B) CNT; (C) nanoG. Experimental values: ●, ○. Values calculated according to the "additive model" (Eq. (11.5)): —. Experimental values: ○ refer to nanocomposites with nanofiller in the neat polymer matrix, ● refer to nanocomposites with nanofiller in the polymer matrix containing 60 phr of CB.
Source: Reprinted with permission from Galimberti M, Cipolletti V, Musto S, Cioppa S, Peli G, Mauro M, et al. Recent advancements in rubber nanocomposites. Rubber Chem Technol 2014;87(3):417−42.

where E(IR) is the measured elastic modulus of the neat IR matrix, $E(\Phi_{CB})$ and $E(\Phi_{nanonanofiller})$ are the moduli of IR composites containing only one filler (CB or nanofiller, respectively). The subscripts refer to the filler content considered, expressed as volume fraction, Φ. Fig. 11.19 shows both the measured and the calculated moduli values for the investigated systems.

For all of the three nanofillers (OC, CNT, and nanoG), interactive effects are shown: the combination of CB and the nanofiller leads to initial modulus values much higher than those calculated through the simple addition of the two initial moduli of the composites containing only CB (60 phr) and only the nanofiller.

However, the systems analyzed do not allow to clarify whether the nanofiller promotes a real synergistic effect, or rather the modulus enhancement is merely due to an increase of the overall filler concentration. Therefore, a further, more systematic work was performed [25] on IR based systems filled with only carbonaceous fillers. Single-filler systems, obtained by adding only CB, CNT, or nanoG at increasing contents were prepared, and, for comparison, also hybrid filler systems were prepared having the same total contents, but made of equal parts of CB and CNT or of CB and nanoG.

The dynamic shear moduli at small deformation amplitude ($G'\gamma_{min}$) were measured and compared to the moduli calculated with the additive rule. The difference between the experimental and the predicted values was labeled "interactive term," $\Delta G'_{int}$. Such a term, indicating the strength of interaction between two fillers with each other, is dependent on the type of matrix and fillers, and on the total and relative filler amount. In order to have reference values for the interactive terms, they were calculated also for single-filler systems, considering the total filler amount (Φ) as made by two equal parts of the same filler (Φ/2) rather than two equal parts of different fillers. Therefore, autointeractive terms indicate the modulus enhancement originated by the interaction between the two parts of the same filler, at the same

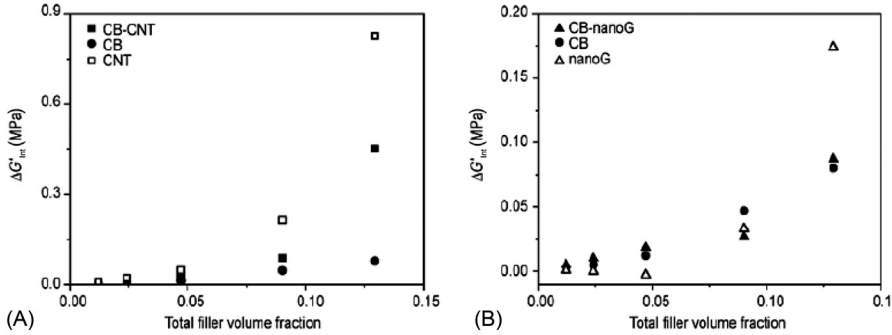

Figure 11.20 Interactive and autointeractive terms as a function of the total filler volume fraction for the investigated systems: (A) CB and/or CNT filled systems; (B) CB and/or nanoG filled systems.
Source: Reprinted with permission from Agnelli S, Cipolletti V, Musto S, Coombs M, Conzatti L, Pandini S, et al. Interactive effects between carbon allotrope fillers on the mechanical reinforcement of polyisoprene based nanocomposites. Express Polym Lett 2014;8 (6):436–49.

total and relative filler volume fractions realized in the hybrid composites. A comparison of interactive and autointeractive terms should evidence the contribution to the interaction term due to the peculiarities of the two different fillers.

Fig. 11.20 shows interactive and autointeractive terms obtained for CB–CNT and CB–nanoG systems as a function of the total filler volume fraction.

CNT promote the highest autointeractive terms, and are responsible for the reinforcement of the hybrid filler system as well: in fact, the interactive terms of the hybrid filler composites with CNT are between those of the single-filler composites, while CB exerts a moderate contribution. On the other hand, nanoG shows a significant autointeractive term only at the highest filler content (33 phr), and it is not able to promote significant interactions with CB in the hybrid filler system, at the contents investigated.

The superior interaction ability of CNT, both with itself and with other particles, was interpreted by the authors with the highest specific surface area of CNT available to the contact with the elastomeric matrix. In fact, by plotting the moduli of single and hybrid filler systems as a function of specific surface area, a common correlation between the reinforcing ability of a nanofiller CNT and a nanostructured filler CB was found. Fig. 11.21 shows such a moduli as a function of the specific surface area, evaluated through Eq. (11.6):

$$\text{Specific surface area (for hybrid fillers)} = A_{\text{CB}} \times \rho_{\text{CB}} \times \Phi_{\text{CB}} + A_{\text{nanofiller}} \times \rho_{\text{nanofiller}} \times \Phi_{\text{nanofiller}} \tag{11.6}$$

where A is assumed to be equal to BET surface area (area per unit of filler weight), ρ is the filler density, and Φ is the filler volume fraction.

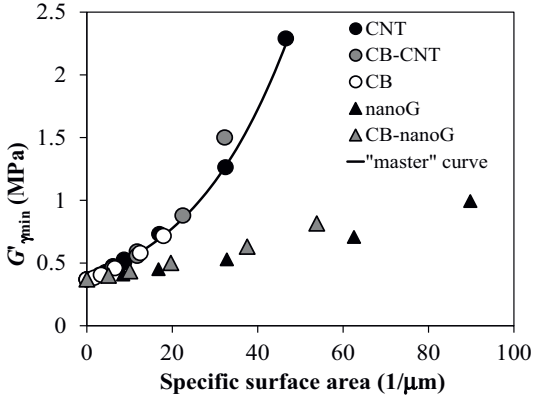

Figure 11.21 Shear modulus as a function of specific surface area for single and hybrid filler systems.
Source: Reprinted with permission from Galimberti M, Cipolletti V, Musto S, Cioppa S, Peli G, Mauro M, et al. Recent advancements in rubber nanocomposites. Rubber Chem Technol 2014;87(3):417−42.

Fig. 11.21 shows also that data of systems filled with nanoG do not lie on the "master" curve common to CNT and CB. The authors attributed this discrepancy to the layered structure of nanoG: the high surface area of filler, measured by gas adsorption method, is not fully accessible to the polymer matrix, lowering its reinforcing efficiency.

Finally, a further analysis was performed by the authors on the systems investigated in [16,25,31,44,78]. The modulus reinforcement promoted by nanofillers was evaluated by a k factor, defined as the ratio of the composite modulus over the matrix modulus. For single-filler composites, the neat polymer was considered as the matrix, for hybrid filler systems, the polymer added with CB was considered as the matrix. Interestingly, by plotting k factors as a function of nanofiller volume fraction, the data for single and hybrid filler composites filled with the same nanofiller are overlapping, as shown in Fig. 11.22.

Although it was not possible to provide a physical motivation for this finding, it is clear that nanofillers enhance the "matrix" modulus by a multiplication factor, k, that depends on the nanofiller type and content, independently of the "matrix" composition, which can be both a neat elastomer and the same elastomer filled with CB.

Such a result brings about also convenient consequences. In fact, provided that the k factor is the same for single and hybrid filler systems, i.e.,

$$k = G'_{\text{nanofiller}}(\Phi_{\text{nanofiller}})/G'_{\text{m}} = G'_{\text{c}}(\Phi_{\text{nanofiller}}, \Phi_{\text{CB}})/G'_{\text{CB}}(\Phi_{\text{CB}}) \tag{11.7}$$

then the modulus of a hybrid filler composite can be calculated as a product of the moduli of the single-filler composites over the matrix modulus. In fact, by rearranging Eq. (11.7), the following relationship is found:

$$G'_{\text{c}}(\Phi_{\text{nanofiller}}, \Phi_{\text{CB}}) = G'_{\text{nanofiller}}(\Phi_{\text{nanofiller}}) * G'_{\text{CB}}(\Phi_{\text{CB}})/G'_{\text{m}} \tag{11.8}$$

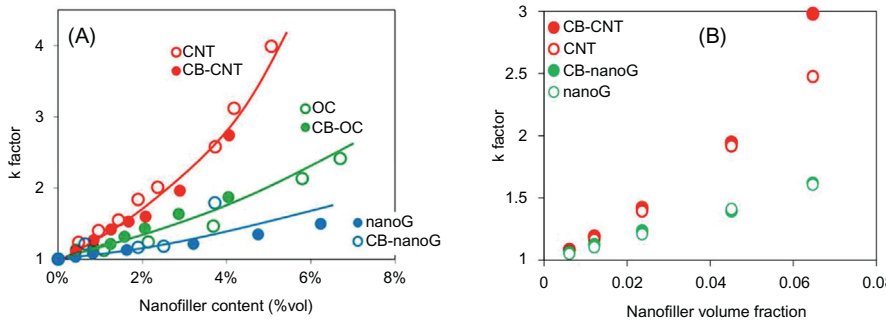

Figure 11.22 *k* factors for nanocomposites containing either OC, CNT, or nanoG as the nanofillers. In both (a and b): in the neat polymer matrix (○). In (A): in the polymer matrix containing 60 phr of CB (●). In (B): in the polymer matrix containing the same amount of CB as the nanofiller (●).

Although limited to the systems investigated by the authors of the chapter, this finding can suggest a general rule for hybrid filler systems, which could help the prediction of the moduli for the hybrid filler composites.

11.7 Hybrid systems made by different nanofillers

Papers are increasingly appearing in the literature on hybrid filler systems based on nanofillers: OC and graphite nanoparticles were combined with CNT. They do not yet allow either a rationalization or even a discussion. However, they already show interesting indications.

As discussed above in this chapter, a relevant issue is the CNT debundling and dispersion in the polymer matrix. The combination of CNTs and lamellar nanoparticles, either graphitic [118] or clays [119], was found to favor CNT dispersion.

A great opportunity is given by the synergistic effect brought about by different types of fillers. Mixed filler networks and consequently synergistic effects on both electrical and mechanical properties were observed with the combination of two graphitic nanofillers, such as CNTs and graphene nanoparticles [120,121]. Synergistic effects were found also from the combination of CNTs and clay on thermal degradation behavior [122] and on mechanical properties [123].

11.8 Conclusions and perspectives

A few words have to be used to summarize the main results reported in previous paragraphs.

Rubber composites based on hybrid filler systems made by nanofillers such as OC, CNT, graphene, and nanographite and nanostructured fillers, such as CB and

silica, do show remarkable improvements in properties compared to composites based on only one family of fillers, i.e., improvements in mechanical reinforcement and electrical and thermal conductivity.

Nano- and nanostructured fillers show synergistic effects, e.g., for the improvement of mechanical properties.

The behavior of nano- and nanostructured fillers can be rationalized upon identifying suitable filler features. For example, a common master curve can be drawn for the improvement of the composite initial modulus as a function of the filler−polymer interfacial area.

List of abbreviations

6PPD	N-(1,3-dimethylbutyl)-N′-phenyl-p-phenylene diamine
AFM	atomic force microscopy
CB	carbon black
CBS	N-cyclohexyl-2-benzothiazole sulfenamide
CDDC	copper dimethyl dithio carbamate
CNTs	carbon nanotubes
CNTBs	carbon nanotube bundles
DCUP	dicumyl peroxide
DSC	differential scanning calorimetry
EPDM	ethylene-propylene diene monomer
FE-SEM	filed emission scanning electron microscopy
IPPD	N-isopropyl-N′-phenyl-p-phenylene diamine
IR	isoprene rubber
MBT	2-Mercaptobenzothiazole
MBTS	2.2′-Dithio-dibenzothiazole
MWCNTs	multiwalled carbon nanotubes
NBR	nitrile-butadiene rubber
NR	natural rubber
PBN	phenyl-β-naphthylamine
phr	per hundred resin
S	sulfur
SA	stearic acid
SBR	styrene-butadiene rubber
sDPA	substituted diphenyl amine
SEM	scanning electron microscopy
SWCNTs	single-walled carbon nanotubes
TAIC	triallyl isocianurate
TBBS	N-tert-butyl-2-benzothiazole sulfenamide
TEM	transmission electron microscopy
TGA	thermogravimetric analysis
TMTD	Bis(dimethylthiocarbamyl) disulfide
TOTM	trioctyl trimellitate 77, 78
WAXD	wide-angle X-ray diffraction

XRD X-ray diffraction
ZDC zinc dithio carbamate
ZDDC zinc dimethyl dithio carbamate
ZDEC zinc diethyl carbamate
ZMMBI zinc methyl mercaptobenzimidazole

References

[1] Donnet JB, Custodero E. Reinforcement of elastomers by particulate fillers. In: Mark JE, Erman B, Eirich FR, editors. The science and technology of rubber. 3rd ed. San Diego: Academic Press; 2005. p. 367–400.

[2] Maiti M, Bhattacharya M, Bhowmick AK. Elastomer nanocomposites. Rubber Chem Technol 2008;81:384–469.

[3] Galimberti M, Cipolletti V, Kumar V. Nanofiller in natural rubber. In: Thomas S, Chan CH, Pothan L, Joy J, Maria H, editors. *Natural rubber materials: volume 2: composites and nanoco*mposites. Royal Society of Chemistry; 2013. p. 34–72.

[4] Vocabulary – Nanoparticles, 2005, PAS 71-2005 BSI.

[5] Ray SS, Okamoto M. Polymer/layered silicate nanocomposites: a review from preparation to processing. Prog Polym Sci 2003;28:1539–641.

[6] Chen B, Evans JRG, Greenwell HC, Boulet P, Coveney PV, Bowden AA, et al. A critical appraisal of polymer–clay nanocomposites. Chem Soc Rev 2008;37:568–94.

[7] Paul DR, Robeson LM. Polymer nanotechnology: nanocomposites. Polymer (Guildf) 2008;49:3187–204.

[8] Galimberti M. Rubber clay nanocomposites: science, technology, applications. 1st ed. John Wiley and Sons; 2011.

[9] Galimberti M. Rubber clay nanocomposites in advanced elastomers - technology, properties and applications. In: Boczkowska A, editor; 2012. p. 91–20. Available from: http://dx.doi.org/0.5772/51410.

[10] Galimberti M, Cipolletti V, Coombs M. Application of clay polymer nanocomposites. In: Bergaya F, Lagaly G, editors. Handbook of clay science. 2nd ed. Amsterdam: Elsevier; 2013 (Part B, Chapter 4.4 ISBN: 9780080993645).

[11] Bokobza L. Multiwall carbon nanotube elastomeric composites: a review. Polymer (Guildf) 2007;48(17):4907–20.

[12] Al-Solamya FR, Al-Ghamdib AA, Mahmoud WE. Piezoresistive behavior of graphite nanoplatelets based rubber nanocomposites. Polym Adv Technol 2012;23(3):478–82.

[13] Bhowmick AK, Bhattacharya M, Mitra S. Exfoliation of nanolayer assemblies for improved natural rubber properties: methods and theory. J Elastom Plast 2010;42(6):517–37.

[14] Bhattacharya M, Maiti M, Bhowmick AK. Tailoring properties of styrene butadiene rubber nanocomposite by various nanofillers and their dispersion. Polym Eng Sci 2009; 49(1):81–98.

[15] Sridhar V, Xu D, Pham TT, Mahapatra SP, Kim JK. Dielectric and dynamic mechanical relaxation behavior of exfoliated nano graphite reinforced flouroelastomer composites. Polym Compos 2009;30(3):334–42.

[16] Galimberti M, Kumar V, Coombs M, Cipolletti V, Agnelli S, Pandini S, et al. Filler networking of a nanographite with a high shape anisotropy and synergism with carbon black in poli(1,4-cis-isoprene) based nanocomposites. Rubber Chem Technol 2014;87 (2):197–218.

[17] McNaught D, Wilkinson A. *IUPAC. compendium of chemical terminology*, (the "Gold Book"). 2nd ed. Oxford: Scientific Publications; 1997XML on-line corrected version: http://goldbook.iupac.org (2006-) created by M. Nic, J. Jirat, B. Kosata; updates compiled by A. Jenkins. ISBN 0-9678550-9-8. Available from: http://dx.doi.org/10.1351/goldbook.
[18] Nanko M. Definitions and categories of hybrid materials. Adv Technol Mater Mater Process 2009;11(1):1–8.
[19] Witt N, Tang Y, Ye L, Fang L. Silicone rubber nanocomposites containing a small amount of hybrid fillers with enhanced electrical sensitivity. Mater Des 2013;45:548–54.
[20] Yan N, Wu JK, Zhan YH, Xia HS. Carbon nanotubes/carbon black synergistic reinforced natural rubber composites. Plast Rubber Compos 2009;38(7):290–6.
[21] Zhan YH, Liu GQ, Xia HS, Yan N. Natural rubber/carbon black/carbon nanotubes composites prepared through ultrasonic assisted latex mixing process. Plast Rubber Compos 2011;40(1):32–9.
[22] Galimberti M, Coombs M, Cipolletti V, Giannini L, Conzatti L. The origin of synergism between an organoclay and carbon black. Appl Clay Sci 2013;83–84:449–56.
[23] Dong B, Liu C, Lu Y, Wu Y. Synergistic effects of carbon nanotubes and carbon black on the fracture and fatigue resistance of natural rubber composites. J Appl Polym Sci 2015;132(25):42075.
[24] Das A, Stoeckelhuber KW, Rooj S, Wang DY, Heinrich G. Synergistic effects of expanded nanoclay and carbon black on natural rubber compound. Kautschuck Gummi Kunstoffe 2010;63(7–8):296–302.
[25] Agnelli S, Cipolletti V, Musto S, Coombs M, Conzatti L, Pandini S, et al. Interactive effects between carbon allotrope fillers on the mechanical reinforcement of polyisoprene based nanocomposites. Express Polym Lett 2014;8(6):436–49.
[26] Jones RG, Ober CK, Hodge P, Kratochvíl P, Moad G, Vert M. Terminology for aggregation and self-assembly in polymer science (IUPAC Recommendations 2013). Pure Appl Chem 2013;85(2):463–92.
[27] Huang JR, Zhu YT, Jiang W, Yin JH, Tang QX, Yang XD. Parallel carbon nanotube stripes in polymer thin film with remarkable conductive anisotropy. ACS Appl Mater Interfaces 2014;6(3):1754–8.
[28] Peng Z, Feng C, Luo Y. Natural rubber/multiwalled carbon nanotube composites developed with a combined self-assembly and latex compounding technique. J Appl Polym Sci 2012;125(5):3920–8.
[29] Yang H, Liu P, Zhang T, Duan Y, Zhang J. Fabrication of natural rubber nanocomposites with high graphene contents via vacuum-assisted self-assembly. RCS Adv 2014;4(53):27687–90.
[30] Zhao Y, Milano G, Cong Y, Yu N, He Y, Cong Y, et al. Self-assembled morphologies and percolation probability of mixed carbon fillers in the diblock copolymer template: hybrid particle-field molecular dynamics simulation. J Phys Chem C 2015;119(44):25009–22.
[31] Galimberti M, Cipolletti V, Musto S, Cioppa S, Peli G, Mauro M, et al. Recent advancements in rubber nanocomposites. Rubber Chem Technol 2014;87(3):417–42.
[32] Jose JP, Thomas S. XLPE based Al_2O_3–clay binary and ternary hybrid nanocomposites: self-assembly of nanoscale hybrid fillers, polymer chain confinement and transport characteristics. Phys Chem Chem Phys 2014;16(37):20190–201.
[33] Wang Q, Li G, Zhang J, Huang F, Lu K, Wei Q. PAN nanofibers reinforced with MMT/GO. J Nanomater 2014; no. 298021.

[34] Konishi Y, Cakmak M. Nanoparticle induced network self-assembly in polymer–carbon black composites. Polymer (Guildf) 2006;47(15):5371–91.
[35] Bao Z, Flanigan C, Beyer L, Tao J. Processing optimization of latex-compounded montmorillonite/styrene-butadiene rubber-polybutadiene rubber. J Appl Polym Sci 2015;132(8):41521/1–41521/8.
[36] Galimberti M, Coombs M, Pandini S, Riccò T, Cipolletti V, Conzatti L, et al. Delamination of organically modified montmorillonite for reducing the filler networking with carbon black in poly(1,4-cis-isoprene) based nanocomposites. Appl Clay Sci 2015;104:8–17.
[37] Nawani P, Burger C, Rong L, Hsiao BS, Tsou AH. Structure and permeability relationships in polymer nanocomposites containing carbon black and organoclay. Polymer (Guildf) 2015;64:19–28.
[38] Annadurai P, Mukundan T, Joseph R. Influence of carbon black in polychloroprene organoclay nanocomposite with improved mechanical, electrical and morphology characteristics. Plast Rubber Compos 2013;42(9):379–84.
[39] Chattopadhyay PK, Praveen S, Das NC, Chattopadhyay S. Contribution of organomodified clay on hybrid microstructures and properties of epoxidized natural rubber-based nanocomposites. Polym Eng Sci 2013;53(5):923–30.
[40] Malas A, Das CK. Selective dispersion of different organoclays in styrene butadiene rubber in the presence of a compatibilizer. Mater Des 2013;49:857–65.
[41] Mohanty TR, Bhandari V, Chandra AK, Chattopadhyay PK, Chattopadhyay S. Role of calcium stearate as a dispersion promoter for new generation carbon black-organoclay based rubber nanocomposites for tyre application. Polym Compos 2013;34(2):214–24.
[42] Sapkota J, Poikelispa M, Das A, Dierkes W, Vuorinen J. Influence of nanoclay-carbon black hybrid fillers on cure and properties of natural rubber compounds. Polym Eng Sci 2013;53(3):615–22.
[43] Sreenivasan P, Ratna D, Albert P, Somashekaran J, Raut R, Chakraborty BC. A new liquid rubber-assisted dispersion of organoclay in carbon black filled carboxylated acrylonitrile–butadiene rubber matrix. J Appl Polym Sci 2013;128(4):2414–23.
[44] Galimberti M, Coombs M, Cipolletti V, Riccio P, Ricco T, Pandini S, et al. Enhancement of mechanical reinforcement due to hybrid filler networking promoted by an organoclay in hydrocarbon based nanocomposites. Appl Clay Sci 2012;65–66:57–66.
[45] Malas A, Das CK. Carbon black–clay hybrid nanocomposites based upon EPDM elastomer. J Mater Sci 2012;47:2016–24.
[46] Chattopadhyay PK, Das NC, Chattopadhyay S. Influence of interfacial roughness and the hybrid filler microstructures on the properties of ternary elastomeric composites. Compos Part A Appl Sci Manuf 2011;42(8):1049–59.
[47] Gopi JA, Patel SK, Chandra AK, Tripathy DK. SBR-clay-carbon black hybrid nanocomposites for tire tread application. J Polym Res 2011;18:1625–34.
[48] Liu Y, Li L, Wang Q, Zhang X. Fracture properties of natural rubber filled with hybrid carbon black/nanoclay. J Polym Res 2011;18:859–67.
[49] Galimberti M, Senatore S, Lostritto A, Giannini L, Conzatti L, Costa G, et al. Reinforcement of diene elastomers by organically modified layered silicates. e-Polymers 2009;1–16 no. 057.
[50] Praveen S, Chattopadhyay PK, Albert P, Dalvi VG, Chakraborty BC, Chattopadhyay S. Synergistic effect of carbon black and nanoclay fillers in styrene butadiene rubber matrix. Development of dual structure. Compos Part A 2009;40:309–16.

[51] Cataldo F. Preparation and properties of nanostructured rubber composites with montmorillonite. Macromol Symp 2007;247:67–77.
[52] Maiti M, Sadhu S, Bhowmick AK. Effect of carbon black on properties of rubber nanocomposites. J Appl Polym Sci 2005;96:443–51.
[53] Galimberti M, Cipolletti V, Giudice S. Morfology of rubber-clay nanocomposites. In: Galimberti M, editor. Rubber clay nanocomposites – science, technology and applications. New York, NY: Wiley and Sons; 2011. p. 181–240.
[54] Cipolletti V, Galimberti M, Mauro M, Guerra G. Organoclays with hexagonal rotator order for the paraffinic chains of the compensating cation. Implications on the structure of clay polymer nanocomposites. Appl Clay Sci 2014;87:179–88.
[55] Lagaly G, Ogawa M, Dekany I. Clay mineral–organic interactions. In: Bergaya F, Lagaly G, editors. *Handbook of* clay *science, Second Edition*. Amsterdam: Elsevier; 2013. p. 435–505.
[56] Herrmann W, Uhl C, Heinrich G, Jehnichen D. Analysis of HNBR-montmorillonite nanocomposites. Morphology, orientation and macroscopic properties. Polym Bull 2006;57:395–405.
[57] Bhattacharya M, Bhowmick AK. Synergy in carbon black-filled natural rubber nanocomposites. Part I: mechanical, dynamic mechanical properties, and morphology. J Mater Sci 2010;45:6126–38.
[58] Kvande I, Øye G, Hammer N, Rønning M, Raaen S, Holmen A, et al. Deposition of Au colloids on plasmachemically modified carbon nanofibers. Carbon N Y 2008;46(5):759–65.
[59] Sabah E, Mart UC, Nar MC, Elik MS. Zeta potentials of sepiolite suspensions in concentrated monovalent electrolites. Sep Sci Technol 2007;42(10):2275–88.
[60] Gates WP. Crystalline swelling of organo-modified clays in ethanol-water solutions. Appl Clay Sci 2004;27:1–12.
[61] Lin JJ, Chu CC, Chiang ML, Tsai WC. First isolation of individual silicate platelets from clay exfoliation and their unique self-assembly into fibrous arrays. J Phys Chem B 2006;110(37):18115–20.
[62] Xu R, Wu C, Xu H. Particle size and zeta potential of carbon black in liquid media. Carbon N Y 2007;45(15):2806–9.
[63] Konishi Y, Cakmak M. Structural hierarchy developed in injection molding of nylon 6/clay/carbon black nanocomposites. Polymer (Guildf) 2005;46(13):4811–26.
[64] Feller JF, Bruzaud S, Grohens Y. Influence of clay nanofiller on electrical and rheological properties of conductive polymer composite. Mater Lett 2004;58(5):739–45.
[65] Thomas S, Stephen R. Rubber nanocomposites: preparation, properties and applications. John Wiley & Sons; 2010.
[66] Semsarzadeh MA, Bakhshandeh GR, Ghasemzadeh-Barvarz M. Effect of carbon black on rate constant and activation energy of vulcanization in EPDM/BR and EPDM/NR blends. Iran Polym J 2005;14(6):573–8.
[67] Avalos F, Ortiz JC, Zitzumbo R, López-Manchado MA, Verdejo R, Arroyo M. Effect of montmorillonite intercalant structure on the cure parameters of natural rubber original research article. Eur Polym J 2008;44(10):3108–15.
[68] Sengupta R, Chakraborty S, Bandyopadhyay S, Dasgupta S, Mukhopadhyay R, Auddy K, et al. A short review on rubber/clay nanocomposites with emphasis on mechanical properties. Polym Eng Sci 2007;47(11):1956–74.
[69] Verdejo R, Hernandez M, Bitinis N, Kenny JM, Lopez-Manchado MA. Vulcanization characteristics and curing kinitects of rubber-organoclay nanocomposites. In: Galimberti M, editor. Rubber clay nanocomposites – science, technology and applications. New York, NY: Wiley and Sons; 2011. p. 275–303.

[70] Giannini L, Citterio A, Galimberti M, Cozzi D. Chemistry of rubber-organoclay nanocomposites. In: Galimberti M, editor. Rubber clay nanocomposites – science, technology and applications. New York, NY: Wiley and Sons; 2011. p. 127–44.
[71] Payne AR, Whittaker RE. Low strain dynamic properties of filled rubbers. Rubber Chem Technol 1971;44(2):440–78.
[72] Medalia AI. Effect of carbon black on dynamic properties of rubber vulcanizates. Rubber Chem Technol 1978;51(3):437–523.
[73] Guth E, Gold O. On the hydrodynamical theory of the viscosity of suspensions. Phys Rev 1938;53:322.
[74] Guth E. Theory of filler reinforcement. Rubber Chem Technol 1945;18(3):595–604.
[75] Huber G, Vilgis TA. Universal properties of filled rubbers: mechanisms for reinforcement on different length scales. Kautschuk Gummi Kunststoffe 1999;52(2):102–7.
[76] Schön F, Gronski W. Filler networking of silica and organoclay in rubber composites: reinforcement and dynamic-mechanical properties. Kautschuk Gummi Kunststoffe 2003;56:166–71.
[77] Ramorino G, Bignotti F, Pandini S, Riccò T. Mechanical reinforcement in natural rubber/organoclay nanocomposites. Compos Sci Technol 2009;69:1206–11.
[78] Galimberti M, Coombs M, Riccio P, Riccò T, Passera S, Pandini S, et al. The role of CNTs in promoting hybrid filler networking and synergism with carbon black in the mechanical behavior of filled polyisoprene. Macromol Mater Eng 2013;298:241–51.
[79] Gelfer M, Burger C, Fadeev A, Sics I, Chu B, Hsiao BS, et al. Thermally induced phase transitions and morphological changes in organoclays. Langmuir 2004;20(9):3746–58.
[80] Osman MA, Ploetze M, Skrabal P. Structure and properties of alkylammonium monolayers self-assembled on montmorillonite platelets. J Phys Chem B 2004;108(8):2580–8.
[81] Vaia RA, Teukolky RK, Giannelis EP. Interlayer structure and molecular environment of alkylammonium layered silicates. Chem Mater 1994;6(7):1017–22.
[82] Klatte SJ, Beck TL. Molecular dynamics of tethered alkanes: temperature-dependent behavior in a high-density chromatographic system. J Phys Chem 1993;97(21):5727–34.
[83] Galimberti M, Guerra G, Lostritto A. Tire and crosslinkable elastomeric composition' European Patent application 2027199 A1 (WO 2007/144012) to Pirelli Tyre S.p.A; 2007.
[84] Galimberti M, Guerra G, Lostritto A, Giannini L. Tire and crosslinkable elastomeric composition European Patent application 2061833 A1 (WO 2008/009304 A1) to Pirelli Tire S.p.A; 2008.
[85] Robertson CG, Lin CJ, Rackaitis M, Roland CM. Influence of particle size and polymer – filler coupling on viscoelastic glass transition of particle-reinforced polymers. Macromolecules 2008;41(7):2727–31.
[86] Qu L, Huang G, Zhang P, Nie Y, Weng G, Wu J. Synergistic reinforcement of nanoclay and carbon black in natural rubber. Polym Int 2010;59(10):1397–402.
[87] Carretero-González J, Retsos H, Verdejo R, Toki S, Hsiao BS, Giannelis EP, et al. Effect of nanoclay on natural rubber microstructure. Macromolecules 2008;41(18):6763–72.
[88] Rattanasom N, Prasertsri S. Relationship among mechanical properties, heat ageing resistance, cut growth behavior and morphology in natural rubber: partial replacement of clay with various types of carbon black at similar hardness level. Polym Test 2009;28(3):270–6.

[89] Galimberti M, Martino M, Guenzi M, Leonardi G, Citterio A. Thermal stability of ammonium salts as compatibilizers in polymer/layered silicate nanocomposites. e-Polymers 2009;1−14 056.
[90] Yunkong P, Kueseng P, Wirasate S, Huynh C, Rattanasom N. Cut growth and abrasion behavior, and morphology of natural rubber filled with MWCNT and MWCNT/carbon black. Polym Test 2015;41:172−83.
[91] Peddini SK, Bosnyak CP, Henderson NM, Ellison CJ, Paul DR. Nanocomposites from styrene -butadiene rubber (SBR) and multiwall carbon nanotubes (MWCNT) part 2: mechanical properties. Polymer (Guildf) 2015;56:443−51.
[92] Thaptong P, Sirisinha C, Thepsuwan U, Sae-Oui P. Properties of natural rubber reinforced by carbon black-based hybrid fillers. Polym Plast Technol Eng 2014;53(8):818−23.
[93] Galimberti M, Coombs M, Cipolletti V, Riccò T, Agnelli S, Pandini S. The role of nanofillers in promoting hybrid filler networking and synergism with carbon black in a hydrocarbon rubber. Kautschuk Gummi Kunstoffe 2013;7−8:31−6.
[94] Ryu S-R, Sung J-W, Lee D-J. Strain-induced crystallization and mechanical properties of NBR composites with carbon nanotube and carbon black. Rubber Chem Technol 2012;85:207−18.
[95] Ismail H, Ramly AF, Othman N. The effect of carbon black/multiwall carbon nanotube hybrid fillers on the properties of natural rubber nanocomposites. Polym Plast Technol Eng 2011;50(7):660−6.
[96] Lorenz H, Fritzsche J, Das A, Stöeckelhuber KW. Advanced elastomer nanocomposites based on CNT-hybrid filler systems. Compos Sci Technol 2009;69:2135−43.
[97] Cataldo F, Ursini O, Angelini G. MWCNTs elastomer nanocomposite, Part 1: the addition of MWCNTs to a natural rubber-based carbon black-filled rubber compound. Fuller Nanotub Carbon Nanostruct 2009;17(1):38−54.
[98] Bokobza L. Mechanical, electrical and spectroscopic investigations of carbon nanotube-reinforced elastomers. Vib Spectrosc 2009;51:52−9.
[99] Bokobza L, Rahmani M, Belin C, Bruneel JL, El Bounia NE. Blends of carbon blacks and multiwall carbon nanotubes as reinforcing fillers for hydrocarbon rubbers. J Polym Sci Part B Polym Phys 2008;46:1939−51.
[100] Mauro M, Cipolletti V, Galimberti M, Longo P, Guerra G. Chemically reduced graphite oxide with improved shape anisotropy. J Phys Chem C 2012;116:24809−13.
[101] Li ZH, Zhang J, Chen SJ. Effects of carbon blacks with various structures on vulcanization and reinforcement of filled ethylene-propylene-diene rubber. Express Polym Lett 2008;2(10):695−704.
[102] Lopez-Manchado MA, Biagiotti J, Valentini L, Kenny JM. Dynamic mechanical and Raman spectroscopy studies on interaction between single-walled carbon nanotubes and natural rubber. J Appl Polym Sci 2004;92:3394−400.
[103] Sui G, Zhong W, Yang X, Zhao S. Processing and material characteristics of a carbon-nanotube-reinforced natural rubber. Macromol Mater Eng 2007;292(9):1020−6.
[104] Shanmugharaj A, Bae J, Lee K, Noh W, Lee S, Ryu S. Physical and chemical characteristics of multiwalled carbon nanotubes functionalized with aminosilane and its influence on the properties of natural rubber composites. Compos Sci Technol 2007;67(9):1813−22.

[105] Falco AD, Marzocca AJ, Corcuera MA, Eceiza A, Mondragon I, Rubiolo GH, et al. Accelerator adsorption onto carbon nanotubes surface affects the vulcanization process of styrene−butadiene rubber composites. J Appl Polym Sci 2009;11(5):2851−7.
[106] Treolar LRG. The physics of rubber elasticity. 3rd ed. Oxford: Clarendon Press; 1975.
[107] Mullins L. Softening of rubber by deformation. Rubber Chem Technol 1969;42(1): 339−62.
[108] Boonstra BB. Reinforcing fillers. In: Blow CM, Hepburn C, editors. *Rubber technology and man*ufacture. London: Butterworths; 1987.
[109] Liu P, Huang Y, Liu CX, Wang Y, Guo XH, Zhang YG, et al. Enhanced electrical conductivity and mechanical stability of flexible pressure-sensitive GNPs/CB/SR composites: synergistic effects of GNPs and CB. J Mater Res Soc 2015;30(22):3394−402.
[110] Yang G, Liao Z, Yang Z, Tang Z, Guo B. Effects of substitution for carbon black with graphene oxide or graphene on the morphology and performance of natural rubber/carbon black composites. J Appl Polym Sci 2015;132(15):41832.
[111] Zhang H, Wang C, Zhang Y. Preparation and properties of styrene-butadiene rubber nanocomposites blended with carbon black-graphene hybrid filler. J Appl Polym Sci 2015;132(3):41309.
[112] Malas A, Pal P, Giri S, Mandal A, Das KC. Synthesis and characterizations of modified expanded graphite/emulsion styrene butadiene rubber nanocomposites: mechanical, dynamic mechanical and morphological properties. Compos Part B 2014;58: 267−74.
[113] Wang LL, Zhang LQ, Tian M. Mechanical and tribological properties of acrylonitrile−butadiene rubber filled with graphite and carbon black. Mater Des 2012;39:450−7.
[114] Raza MA, Westwood A, Stirling C. Carbon black/graphite nanoplatelet/rubbery epoxy hybrid composites for thermal interface applications. J Mater Sci 2012;47:1059−70.
[115] Park SM, Lim YW, Kim CH, Kim DJ, Moon WJ, Kim JH, et al. Effect of carbon nanotubes with different lengths on mechanical and electrical properties of silica-filled styrene butadiene rubber compounds. J Ind Eng Chem 2013;19:712−19.
[116] Fritzsche J, Lorenz H, Klueppel M. CNT based elastomer-hybrid-nanocomposites with promising mechanical and electrical properties. Macromol Mater Eng 2009;294:551−60.
[117] Sternstein SS, Ramorino G, Jang B, Zhu A-J. Reinforcement and nonlinear viscoelasticity of polymer melts containing mixtures of nanofillers. Rubber Chem Technol 2005;78:258−70.
[118] Hu H, Zhao L, Liu J, Liu Y, Cheng J, Luo J, et al. Enhanced dispersion of carbon nanotube in silicone rubber assisted by graphene. Polymer (Guildf) 2012;53:3378−85.
[119] Rooj S, Das A, Stöckelhuber KW, Wießner S, Fischer D, Reuter U, et al. Expanded organoclay' assisted dispersion and simultaneous structural alterations of multiwall carbon nanotube (MWCNT) clusters in natural rubber. Compos Sci Technol 2015;107:36−43.
[120] Das A, Kasaliwal GR, Jurk R, Boldt R, Fischer D, Stöckelhuber KW, et al. Rubber composites based on graphene nanoplatelets, expanded graphite, carbon nanotubes and their combination: a comparative study. Compos Sci Technol 2012;72:1961−7.
[121] Ponnamma D, Sadasivuni KK, Strankowski M, Guob Q, Thomas S. Synergistic effect of multi walled carbon nanotubes and reduced graphene oxides in natural rubber for sensing application. Soft Matter 2013;9:10343−53.
[122] Chen S, Yu H, Ren W, Zhan Y. Thermal degradation behavior of hydrogenated nitrile-butadiene rubber (HNBR)/clay nanocomposite and HNBR/clay/carbon nanotubes nanocomposites. Thermochimica Acta 2009;491:103−8.

[123] Ivanoska-Dacikj A, Bogoeva-Gaceva G, Rooj S, Wießner S, Heinrich G. Fine tuning of the dynamic mechanical properties of natural rubber/carbon nanotube nanocomposites by organically modified montmorillonite: a first step in obtaining high-performance damping material suitable for seismic application. Appl Clay Sci 2015; 118:99−106.

[124] Osman MA, Ernst M, Meier BH, Suter UW. Structure and molecular dynamics of alkane monolayers self-assembled on mica platelets. J Phys Chem B 2002;106(3): 653−62.